

COMPUTATIONAL ANALYSIS OF EFFECTS OF OPTICAL SOURCE
HAVING RANDOM PHASE ON THE DATA TRANSFER IN FREE SPACE
OPTICS SYSTEMS

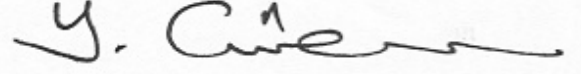
A THESIS SUBMITTED TO
THE GRADUATE SCHOOL OF NATURAL AND APPLIED SCIENCES
OF
ÇANKAYA UNIVERSITY

BY
ALİ BİLGE GÜVENÇ

IN PARTIAL FULFILMENT OF THE REQUIREMENTS FOR THE
DEGREE OF MASTER OF SCIENCE
IN
THE DEPARTMENT OF COMPUTER ENGINEERING

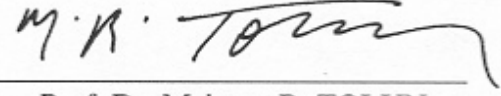
JANUARY 2006

Approval of the Graduate School of Natural and Applied Sciences



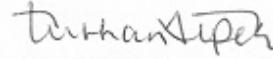
Prof. Dr. Yurdahan GÜLER
Director

I certify that this thesis satisfies all the requirements as a thesis for the degree of Master of Science.



Prof. Dr. Mehmet R. TOLUN
Chairman of the Department

This is to certify that we have read this thesis and that in our opinion it is fully adequate, in scope and quality, as a thesis for the degree of Master of Science.



Prof. Dr. Turhan ALPER
Supervisor

Examining Committee Members

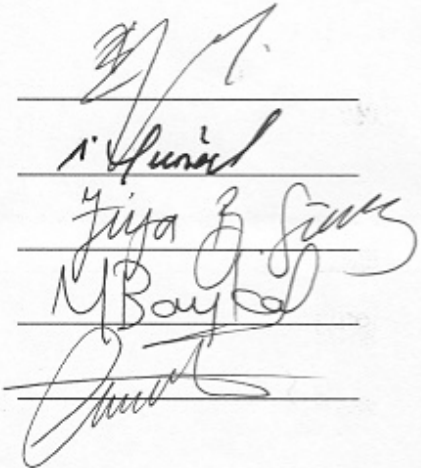
Prof. Dr. Erdem YAZGAN

Prof. Dr. İbrahim GÜNAL

Prof. Dr. Ziya B. GÜVENÇ

Prof. Dr. Yahya K. BAYKAL

Yrd. Doç. Dr. Cem ÖZDOĞAN



ABSTRACT

COMPUTATIONAL ANALYSIS OF EFFECTS OF OPTICAL SOURCE
HAVING RANDOM PHASE ON THE DATA TRANSFER IN FREE SPACE
OPTICS SYSTEMS

Güvenç, Ali Bilge

M. Sc., Department of Computer Engineering

Supervisor: Prof. Dr. Turhan Alper

January 2006, 73 pages

This study describes the effects of spatial random source phase and atmospheric turbulence on the laser intensity profile of a Free Space Optics system. The work is done in two steps. First, effects of the received intensity variations is studied for the speckle (in the absence of atmosphere), then atmospheric turbulence is introduced to simulation to examine the intensity profiles in the atmospheric optical link. At the end, the performance of an FSO system is examined depending on these effects.

Keywords: Free Space Optics, Spatial Random Phase, Atmospheric Turbulence

ÖZ

RASGELE FAZLI OPTİK KAYNAKLARIN SERBEST UZAY OPTİK SİSTEMLERDE VERİ İLETİMİ ÜZERİNDEKİ ETKİSİNİN BİLGİSAYAR ANALİZİ

Güvenç, Ali Bilge

Yüksek Lisans, Bilgisayar Mühendisliği

Tez Yöneticisi: Prof. Dr. Turhan Alper

Ocak 2006, 73 sayfa

Bu çalışma, uzaysal rasgele kaynak fazının ve atmosferik türbülansın Serbest Uzay Optik bir sistemin lazer yoğunluk profili üzerindeki etkilerini incelemektedir. Bu iş iki adımda gerçekleştirilmektedir. İlk olarak, alıcıdaki ışık şiddeti değişimlerinin etkisi speckle için (atmosfer olmadığı durumda) incelenmiş, daha sonra atmosferik optik link'deki ışık şiddeti profillerini incelemek için atmosferik türbülans simülasyona dahil edilmiştir. Sonuç olarak, bu etkilere bağlı olarak Serbest Uzay Optik bir sistemin performansı incelenmektedir.

Anahtar Kelimeler: Serbest Uzay Optik, Uzaysal Faz, Atmosferik Türbülans

ACKNOWLEDGMENTS

I express my sincere appreciation to my supervisor Prof. Dr. Turhan ALPER for his valuable comments, suggestions and contributions.

I would like to thank Prof. Dr. Yahya Kemal BAYKAL for his guidance, support and encouragement throughout this study.

Finally, I offer my sincere thanks to my family for their understanding and support they provided during this study.

TABLE OF CONTENTS

ABSTRACT	i
ÖZ.....	ii
ACKNOWLEDGMENTS.....	iii
TABLE OF CONTENTS	iv
LIST OF FIGURES.....	vi
CHAPTER 1.....	1
INTRODUCTION.....	1
1.1 Free Space Optics.....	1
1.2 Atmospheric Effects on FSO Systems	2
1.3 Laser Wavelength Selection for FSO.....	4
CHAPTER 2.....	5
ELECTROMAGNETIC WAVE PROPAGATION.....	5
2.1 Introduction	5
2.2 Wave Equation	5
2.3 The Three-Dimensional Wave Equation.....	9
2.4 Optical Waves in Free Space.....	10
2.5 Plane Waves	12
2.6 Spherical Waves.....	15
CHAPTER 3.....	18
HUYGENS – FRESNEL AND FIELD INTEGRAL.....	18
3.1 Introduction	18
3.2 The Huygens - Fresnel Principle.....	18

3.3	Laser Intensity	31
3.4	Spatial Random Source Phase	33
3.5	Parameters of Atmospheric Turbulence	35
CHAPTER 4		38
SIMULATION		38
4.1	Introduction	38
4.2	Numerical Integration of Field Integral	38
4.3	Simulation Results	41
CHAPTER 5		54
CONCLUSION		54
REFERENCES		57
APPENDIX A : Intensity Profile		59
APPENDIX B : Field Integrand		66
APPENDIX C : Gauss Quad		67
APPENDIX D : Intensity Level		69
APPENDIX E : Comparison		72

LIST OF FIGURES

Figure 2-1 : Transverse displacement of a string. The segment between x and $x + \Delta x$ is acted upon by the tensions T along the tangent to the string at both ends.....	6
Figure 3-1 : Diffraction by two pinholes in a screen.....	22
Figure 3-2 : Spherical wave propagation.	25
Figure 3-3 : Derivation of Huygens-Fresnel diffraction integrals.....	25
Figure 3-4 : Probability Density Function of spatial random source phase.	34
Figure 3-5 : Propagation of field on x_0, y_0 plane and integration point on field...	34
Figure 4-1 : Laser intensity profile of FSO system using 1550nm wavelength laser for a 2000m propagation distance. Random source phase and atmospheric turbulence are not included.....	42
Figure 4-2 : Laser Intensity profile of FSO system using 1550nm wavelength laser for a 5000m propagation distance. Random source phase and atmospheric turbulence are not included.....	42
Figure 4-3 : Laser beam spread of FSO system using 1550nm wavelength laser due to propagation distance. Random source phase and atmospheric turbulence are not included.....	43
Figure 4-4 : Laser Intensity profile of FSO system using 1550nm wavelength laser for a 2000m propagation distance. Random source phase included and expansion coefficient is π	44
Figure 4-5 : Laser Intensity profile of FSO system using 1550nm wavelength laser for a 2000m propagation distance. Random source phase included and expansion coefficient is 2π	44

Figure 4-6 : Laser Intensity profile of FSO system using 1550nm wavelength laser for a 3000m propagation distance. Random source phase included and expansion coefficient is π	45
Figure 4-7 : Laser Intensity profile of FSO system using 1550nm wavelength laser for a 3000m propagation distance. Random source phase included and expansion coefficient is 2π	45
Figure 4-8 : Laser Intensity profile of FSO system using 1550nm wavelength laser for a 5000m propagation distance. Random source phase included and expansion coefficient is π	46
Figure 4-9 : Laser Intensity profile of FSO system using 1550nm wavelength laser for a 5000m propagation distance. Random source phase included and expansion coefficient is 2π	46
Figure 4-10 : Comparison of laser beam spread of FSO system using 1550nm wavelength laser for a 2000m-5000m propagation distance due to the expansion coefficient of the random source phase.....	47
Figure 4-11 : Laser Intensity profile of FSO system using 1550nm wavelength laser for a 2000m propagation distance. Random source phase included and expansion coefficient is π . Atmospheric turbulence is included.....	48
Figure 4-12 : Laser Intensity profile of FSO system using 1550nm wavelength laser for a 2000m propagation distance. Random source phase included and expansion coefficient is 2π . Atmospheric turbulence is included.....	48
Figure 4-13 : Laser Intensity profile of FSO system using 1550nm wavelength laser for a 3000m propagation distance. Random source phase included and expansion coefficient is π . Atmospheric turbulence is included.....	49

Figure 4-14 : Laser Intensity profile of FSO system using 1550nm wavelength laser for a 3000m propagation distance. Random source phase included and expansion coefficient is 2π . Atmospheric turbulence is included.....	49
Figure 4-15 : Laser Intensity profile of FSO system using 1550nm wavelength laser for a 5000m propagation distance. Random source phase included and expansion coefficient is π . Atmospheric turbulence is included.....	50
Figure 4-16 : Laser Intensity profile of FSO system using 1550nm wavelength laser for a 5000m propagation distance. Random source phase included and expansion coefficient is 2π . Atmospheric turbulence is included.....	50
Figure 4-17 : Comparison of laser beam spread of FSO system using 1550nm wavelength laser for a 2000m-5000m propagation distance due to the expansion coefficient of the random source phase.....	51
Figure 4-18 : Comparison of laser beam spread of FSO system for random source phase with atmospheric turbulence and random source phase without atmospheric turbulence for a 2000m propagation distance due to the expansion coefficient of the random source phase.....	52
Figure 4-19 : Comparison of laser beam spread of FSO system for random source phase with atmospheric turbulence and random source phase without atmospheric turbulence for a 3000m propagation distance due to the expansion coefficient of the random source phase.....	52

Figure 4-20 : Comparison of laser beam spread of FSO system for random source phase with atmospheric turbulence and random source phase without atmospheric turbulence for a 5000m propagation distance due to the expansion coefficient of the random source phase..... 53

Figure 5-1 : Comparison of laser intensity on receiver site due to expansion coefficient of the spatial random source phase for propagation distances from 2000m up to 5000m. 54

CHAPTER 1

INTRODUCTION

1.1 Free Space Optics

Free Space Optics (FSO), also called Free Space Photonics (FSP) or Optical Wireless, refers to the transmission of modulated visible or infrared (IR) beams through the atmosphere to obtain broadband communications [1]. FSO systems are used to transmit voice, data and video up to 5km distances. Communication with FSO systems is possible as long as there is a clear line of sight between the source and the destination. Some of the applications of Free Space Optics systems are;

Providing broadband communication wherever line-of-sight exists and cable-less access solutions are not available or are too expensive. Therefore with the advantages of high-speed and rapid deployment wireless links, FSO overcomes limitations of traditional radio wireless networks, ADSL, VDSL and cable modem solutions

Used in first- or last-mile carrier applications, and in GSM, GPRS and 3G wireless networks.

Used in Metropolitan Area Networks (MAN) where clients can extend existing infrastructure or entirely bypass local-loop connections. Mesh, Ring and Star network topologies are used to provide high availability solutions.

1.2 Atmospheric Effects on FSO Systems

The atmosphere of the earth affects the transmission of all types of electromagnetic radiation used to provide communications through the atmosphere. Radio, microwave and FSO systems are affected to different degrees by weather due primarily to the differences in wavelength. An FSO signal propagating through the earth's atmosphere is subject to attenuation and distortion due to absorption and scattering by aerosols such as fog, and to due to absorption and scattering by molecules, and due to atmospheric turbulence. All three conditions can degrade the received light energy [2].

Molecular Absorption is caused mainly by the water vapor, carbon dioxide and ozone content of the air along the transmission path. As long as the correct wavelength is chosen molecular absorption is not an issue with FSO systems. There are good transmission windows, greater than ninety percent transmittance, at both the 810nm and 1550nm wavelengths that are commonly used in FSO systems [3].

Scattering has a much greater effect than absorption. The atmospheric scattering of light is a function of its wavelength and the number and size of scattering particles in the air. The optical visibility along the path is directly related to the number and size of these particles [2]. Visibility distance is defined as the distance that the human eye can just distinguish a one meter square black target against a white background.

Scattering is caused when the wavelength collides with the particles such as fog and smoke. The physical size of the particle determines the type of scattering. When the particle is smaller than the wavelength, this is known as Rayleigh

scattering. When the particle is of comparable size to the wavelength, this is known as Mie scattering. When the particle is much larger than the wavelength, this is known as non-selective scattering. In scattering, there is no loss of energy, only a directional redistribution of energy that may have significant reduction in beam intensity for longer distances.

Atmospheric Turbulence is the subject of which its effect is simulated in chapter 4. The visual distortion of images seen looking down a hot asphalt road is known as shimmer, or atmospheric turbulence. Turbulence is a function of time of daytime heating terrain, cloud cover, wind, and height of the beam path above the source of turbulence. Beam scintillation is the most common form of atmospheric turbulence [4].

The index of refraction of air is dependent upon the temperature. Because the refraction index along the path changes, at receiver beam having random amplitude and phase is received.

Beam scintillation is a small-scale destructive interference within the beam's cross section which causes variations in the power density at the receiver. Beam scintillation creates a random fading in the carrier beam intensity which causes the signal amplitude decrease below the threshold values and error or complete lost of communication for short terms.

Atmospheric turbulence introduces quite complex variations. However, it can usually be dealt with by proper system design, mounting precautions and sight selection.

1.3 Laser Wavelength Selection for FSO

Laser communications systems should be designed to be eye-safe, which means that they cause no danger to people who might encounter the communications beam. Laser eye safety is classified by the International Electro-technical Commission (IEC). A laser transmitter that is completely safe when viewed by the unaided eye is designated IEC Class 1M.

The eye-safe limits vary with wavelength. Commercially available optical wireless hardware can be classified into two categories. First, systems that operate at a wavelength near 800 nm and second, systems that operate near 1550 nm. Laser beams at 800 nm are near-infrared and therefore invisible so like visible wavelengths, the light passes through the cornea and lens and is focused onto a tiny spot on the retina which applies for visible and near-infrared wavelengths in the range of 400 to 1400 nm [5]. The light beam entering the eye in this retinal-hazard wavelength region is concentrated by a factor of 100,000 times when it strikes the retina. Thus, at 800 nm the retina could be permanently damaged by some commercially available optical-wireless products before the victim is aware. However, laser beams at wavelengths greater than 1400 nm are absorbed by the cornea and lens, and do not focus onto the retina. Because of this, wavelengths greater than 1400 nm are allowed approximately 50 times greater intensities than wavelengths near 800 nm. This fact can be used by specifying a wavelength in the 1550 nm range because using fifty times larger laser power allows the laser to propagate over longer distances and higher data rates [2].

In order to fulfill the requirements discussed above in commercially available devices 1550 nm is used as the wavelength of laser so in the simulation of thesis the wave length is selected as 1550 nm.

CHAPTER 2

ELECTROMAGNETIC WAVE PROPAGATION

2.1 Introduction

In this chapter, electromagnetic propagation is studied. The basic concepts of theory and basic formulas are given for electromagnetic wave propagation. The theory is investigated for wave equation and wave propagation.

2.2 Wave Equation

Small transverse displacements, s , obey the one-dimensional wave equation, as the propagation of a transverse disturbance or a transverse wave is assumed to lie always in a plane [6].

$$\frac{\partial^2 s}{\partial x^2} - \frac{1}{c^2} \frac{\partial^2 s}{\partial t^2} = 0 \quad (2.1)$$

Here c represents the speed of the waves. This equation has quite general applicability.

The displacement of the string from equilibrium $s(x, t)$ is plotted [7] as a function of x for a particular values the time t in figure 2-1.

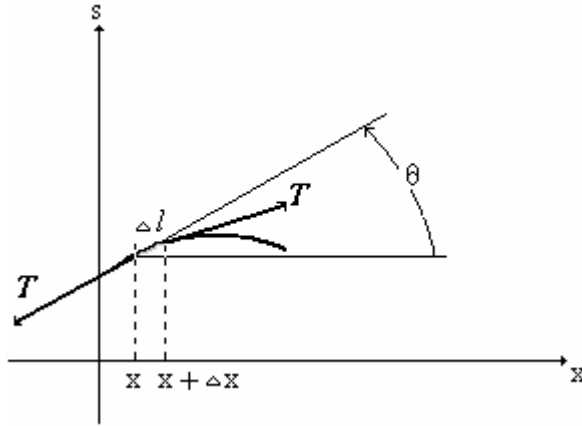


Figure 2-1 : Transverse displacement of a string. The segment between x and $x + \Delta x$ is acted upon by the tensions T along the tangent to the string at both ends.

To derive equation (2.1) for the string, we begin by applying Newton's second law of motion to a small section of the string of length Δl located between x and $x + \Delta x$, as shown in figure 2-1. At any given point the tension always acts along the tangent to the string. The angle θ between tangent and the axis can be obtained from

$$\tan \theta = \frac{\partial s}{\partial x} \quad (2.2)$$

Making the necessary assumption that the angle θ measured in radians is small compared with unity;

$$|\theta| \ll 1 \quad (2.3)$$

This allows us to make these approximations:

$$\sin \theta \approx \tan \theta \approx \theta \quad (2.4)$$

and

$$\cos \theta \approx 1 \quad (2.5)$$

The horizontal and vertical magnitudes are given below as θ being the angle between tangent and the axis at a given point.

$$T_{hor} = T \cos \theta \approx T, \text{ a constant} \quad (2.6)$$

and

$$T_{vert} = T \sin \theta \approx T \tan \theta = T \frac{\partial s}{\partial x} \quad (2.7)$$

The last equation follows from equation (2.2).

The clear horizontal force on the given part of string is then zero which means that there is no acceleration in the x direction but there is a clear vertical force which is given by

$$F_{vert} = T \frac{\partial s}{\partial x}(x + \Delta x, t) - T \frac{\partial s}{\partial x}(x, t) \quad (2.8)$$

If we simplify above equation (2.8) to $(\mu \Delta x a_c / \cos \theta) \approx \mu \Delta x a_c$ which is also known as the motion equation, where μ is the mass per unit length of the string

and a_c is the vertical or transverse component of acceleration of the center of the segment. Then it becomes approximately;

$$a_c = \frac{\partial^2 s}{\partial x^2} \left(x + \frac{\Delta x}{2}, t \right) \quad (2.9)$$

Combining equations (2.8) and (2.9) into the equation of motion gives

$$T \left[\frac{\partial s}{\partial x} (x + \Delta x, t) - \frac{\partial s}{\partial x} (x, t) \right] = \mu \Delta x \frac{\partial^2 s}{\partial x^2} \left(x + \frac{1}{2} \Delta x, t \right) \quad (2.10)$$

If we divide equation (2.10) by Δx and take the limit of this as Δx goes to zero, which allows us to apply the definition of derivative and obtain

$$T \frac{\partial^2 s}{\partial x^2} = \mu \frac{\partial^2 s}{\partial t^2} \quad (2.11)$$

Equation (2.11) is of the form of (2.1) provided that

$$c^2 = \frac{T}{\mu} \quad (2.12)$$

2.3 The Three-Dimensional Wave Equation

In three dimensions the wave equation (2.1)

$$\frac{\partial^2 s}{\partial x^2} - \frac{1}{c^2} \frac{\partial^2 s}{\partial t^2} = 0 \quad (2.13)$$

can be generalized to

$$\frac{\partial^2 \rho}{\partial x^2} + \frac{\partial^2 \rho}{\partial y^2} + \frac{\partial^2 \rho}{\partial z^2} - \frac{1}{c^2} \frac{\partial^2 \rho}{\partial t^2} = 0 \quad \text{or} \quad \nabla^2 \rho - \frac{1}{c^2} \frac{\partial^2 \rho}{\partial t^2} = 0 \quad (2.14)$$

Here ∇ is known as the vector differential operator “dell”. The coefficients in Cartesian coordinate system are given by $(\partial/\partial x, \partial/\partial y, \partial/\partial z)$, and ∇^2 is an abbreviation for the inner product or dot product of ∇ with itself: $\nabla \cdot \nabla = \nabla^2 = (\partial^2/\partial x^2 + \partial^2/\partial y^2 + \partial^2/\partial z^2)$. The function $\rho(x, y, z, t)$ could represent one of several physical quantities that can obey equation (2.14) [7].

Light consists of electromagnetic waves. In free space each spatial component of electric field \mathbf{E} and the magnetic flux density \mathbf{B} obeys an equation of the form of a three-dimensional wave equation given in equation (2.14). In addition to satisfy the wave equation, \mathbf{E} and \mathbf{B} must satisfy the electromagnetic theory known as Maxwell’s equations which will be discussed in section 2.4. These extra equations means that for the individual elementary sinusoidal components of the waves, vectors \mathbf{E} and \mathbf{B} must be mutually perpendicular and also perpendicular to the direction of propagation. This transverse nature of light waves gives rise to the various phenomena associated with the term polarization [7]. In the theory, the

vector nature of optical disturbance is the vector nature of \mathbf{E} and \mathbf{B} and it is treated as a scalar.

2.4 Optical Waves in Free Space

If we apply Maxwell's equations which are known as the equations of electromagnetic theory to a charge and current free region, as a result we get three-dimensional wave equation.

In free space, the four Maxwell's equations are given as;

$$\nabla \cdot \mathbf{E} = 0 \quad (2.15)$$

$$\nabla \cdot \mathbf{B} = 0 \quad (2.16)$$

$$\nabla \times \mathbf{B} = \frac{1}{c} \frac{\partial \mathbf{E}}{\partial t} \quad (2.17)$$

$$\nabla \times \mathbf{E} = -\frac{1}{c} \frac{\partial \mathbf{B}}{\partial t} \quad (2.18)$$

We use c.g.s. Gaussian units. The symbol $c=3 \times 10^8$ m/sec. is the velocity of light in vacuum. The electric field \mathbf{E} is in statvolts/cm or dynes/stat-coulomb. The magnetic induction \mathbf{B} is in gauss [7].

If we take the curl of both sides of the curl \mathbf{E} equation we get the derivation of the wave equation given below;

$$\nabla \times (\nabla \times \mathbf{E}) = \nabla(\nabla \cdot \mathbf{E}) - \nabla^2 \mathbf{E} = -\nabla^2 \mathbf{E} \quad (2.19)$$

The equation (2.19) holds because $\nabla \cdot \mathbf{E} = 0$. Then

$$-\nabla^2 \mathbf{E} = -\frac{1}{c} \frac{\partial}{\partial t} (\nabla \times \mathbf{B}) \quad (2.20)$$

Then use the curl \mathbf{B} equation from (2.15-to-18).

$$-\nabla^2 \mathbf{E} = -\frac{1}{c^2} \frac{\partial^2 \mathbf{E}}{\partial t^2} \quad (2.21)$$

or

$$\nabla^2 \mathbf{E} - \frac{1}{c^2} \frac{\partial^2 \mathbf{E}}{\partial t^2} = 0 \quad (2.22)$$

In a similar way, if we take the curl of the curl \mathbf{B} equation we get;

$$\nabla \times (\nabla \times \mathbf{B}) = \nabla(\nabla \cdot \mathbf{B}) - \nabla^2 \mathbf{B} = -\nabla^2 \mathbf{B} \quad (2.23)$$

and then make use of the curl \mathbf{E} equation to obtain

$$\nabla^2 \mathbf{B} - \frac{1}{c^2} \frac{\partial^2 \mathbf{B}}{\partial t^2} = 0 \quad (2.24)$$

Therefore each component of \mathbf{B} and \mathbf{E} obeys the usual three-dimensional wave equation

$$\nabla^2 \mathbf{E}_x - \frac{1}{c^2} \frac{\partial^2 \mathbf{E}_x}{\partial t^2} = 0 \quad (2.25)$$

These equations given above and their solutions are all dependent to each other because of Maxwell's equations given in equation (2.15-to-18).

2.5 Plane Waves

If we assume that ρ is a function of x and t , a simple situation comes through. That means, we reduce equation (2.14) to equation (2.1) and have the same general solution;

$$\rho(x,t) = f\left(t - \frac{x}{c}\right) + g\left(t + \frac{x}{c}\right) \quad (2.26)$$

In this situation the propagating wave is constant over each yz plane and consists of two parts. First part is propagating along $+x$ axis with the velocity magnitude c which is the f term and the second one is propagating along the $-x$ axis with velocity magnitude c which is the g term.

Consider a special case of equation (2.26) which is a sinusoidal traveling plane wave and g is assumed to be zero;

$$\rho(x,t) = f\left(t - \frac{x}{c}\right) = A \cos\left[2\pi\nu\left(t - \frac{x}{c}\right) + \phi\right] \quad (2.27)$$

Here A is called the amplitude of the wave, ν the frequency (in cycles per second), and ϕ the constant phase angle. The frequency is generally shown in angular form that;

$$w = 2\pi\nu \quad (2.28)$$

and measured in radians per second. Equation (2.27) can also be written as

$$\rho(x,t) = A \cos\left(wt - \frac{2\pi x}{\lambda} + \phi \right) = A \cos(wt - kx + \phi) \quad (2.29)$$

Where λ is the wavelength and given by

$$\lambda = \frac{c}{\nu} \quad (2.30)$$

and represents the crest-to-crest or trough-to-trough spatial distance between waves at a given time [7]. The parameter $k = 2\pi / \lambda$ is called the wave number.

The total argument of the cosine function is shown below

$$\left[2\pi\nu\left(t - \frac{x}{c} \right) + \phi \right] - \left(wt - \frac{2\pi x}{\lambda} + \phi \right) = (wt - kx + \phi) \quad (2.31)$$

which represents the total phase at x and t . For the case of a wave propagating in the $+x$ direction, the total phase increases with time at a given point. Also it decreases linearly with x at a given time.

Expressions like equation (2.2) can be written in order to describe uniform disturbances over the xz plane propagating along the $+y$ or $-y$ axis or uniform disturbances over the xy plane propagating along the $+z$ or $-z$ axis.

If the normal to the plane of the propagating wave is not along a coordinate axis, but along a direction of unit vector $\mathbf{n} = (n_x, n_y, n_z)$, a general plane wave propagating in the $+\mathbf{n}$ direction can be written in the form

$$\rho(\mathbf{r}, t) = f\left(t - \frac{\mathbf{r} \cdot \mathbf{n}}{c}\right) = f\left(t - \frac{xn_x + yn_y + zn_z}{c}\right) \quad (2.32)$$

The above equation (2.32) is a solution of equation (2.14). In order to obtain the same structure first,

$$\frac{\partial f}{\partial x} = -\frac{n_x}{c} f' \quad (2.33)$$

and then

$$\frac{\partial^2 f}{\partial x^2} = -\frac{n_x^2}{c^2} f'' \quad (2.34)$$

it becomes in the form

$$\frac{\partial^2 f}{\partial x^2} + \frac{\partial^2 f}{\partial y^2} + \frac{\partial^2 f}{\partial z^2} = \frac{n_x^2 + n_y^2 + n_z^2}{c^2} f'' = \frac{1}{c^2} f'' = \frac{1}{c^2} \frac{\partial^2 f}{\partial t^2} \quad (2.35)$$

According to the definition of equation (2.32), this gives a constant value for the disturbance ρ at a given value of time for all values of the position vector \mathbf{r} obeying $\mathbf{r} \cdot \mathbf{n} = \text{const}$. Such an equation defines a plane perpendicular to \mathbf{n} . As the value of $\mathbf{r} \cdot \mathbf{n}$ increases algebraically, the plane moves in the $+\mathbf{n}$ [7].

The general expressions for a disturbance moving in the $-\mathbf{n}$ direction is

$$\rho(r,t) = g\left(t + \frac{\mathbf{r} \cdot \mathbf{n}}{c}\right) \quad (2.36)$$

2.6 Spherical Waves

If we assume that the function $\rho(\mathbf{r},t)$ has a spherical symmetry about the origin, another simple solution of three-dimensional wave equation comes through.

$$\rho(\mathbf{r},t) = \rho(r,t) \quad (2.37)$$

Only, where

$$r = \sqrt{x^2 + y^2 + z^2} \quad (2.38)$$

To calculate $\nabla^2 \rho$ in case we begin with

$$\frac{\partial \rho}{\partial x} = \frac{\partial \rho(r,t)}{\partial r} \frac{\partial r}{\partial x} = \left(\frac{\partial \rho}{\partial r}\right) \frac{x}{r} \quad (2.39)$$

and differentiate once more to obtain

$$\frac{\partial^2 \rho}{\partial x^2} = \frac{\partial}{\partial x} \left(\frac{x}{r} \frac{\partial \rho}{\partial r} \right) = \frac{1}{r} \frac{\partial \rho}{\partial r} + x \frac{\partial}{\partial x} \left(\frac{1}{r} \frac{\partial \rho}{\partial r} \right) \quad (2.40)$$

$$= \frac{1}{r} \frac{\partial \rho}{\partial r} + x \frac{\partial}{\partial x} \left(\frac{1}{r} \frac{\partial \rho}{\partial r} \right) \frac{\partial r}{\partial x} \quad (2.41)$$

$$= \frac{1}{r} \frac{\partial \rho}{\partial r} + \frac{x^2}{r} \left(-\frac{1}{r^2} \frac{\partial \rho}{\partial r} + \frac{1}{r} \frac{\partial^2 \rho}{\partial r^2} \right) \quad (2.42)$$

$$\frac{\partial^2 \rho}{\partial x^2} = \frac{1}{r} \frac{\partial \rho}{\partial r} - \frac{x^2}{r^3} \frac{\partial \rho}{\partial r} + \frac{x^2}{r^2} \frac{\partial^2 \rho}{\partial r^2} \quad (2.43)$$

In the same way we obtain the other derivatives:

$$\frac{\partial^2 \rho}{\partial y^2} = \frac{1}{r} \frac{\partial \rho}{\partial r} - \frac{y^2}{r^3} \frac{\partial \rho}{\partial r} + \frac{y^2}{r^2} \frac{\partial^2 \rho}{\partial r^2} \quad (2.44)$$

$$\frac{\partial^2 \rho}{\partial z^2} = \frac{1}{r} \frac{\partial \rho}{\partial r} - \frac{z^2}{r^3} \frac{\partial \rho}{\partial r} + \frac{z^2}{r^2} \frac{\partial^2 \rho}{\partial r^2} \quad (2.45)$$

If we calculate the summation of three equations

$$\nabla^2 \rho = \frac{3}{r} \frac{\partial \rho}{\partial r} - \frac{(x^2 + y^2 + z^2)}{r^3} \frac{\partial \rho}{\partial r} + \frac{(x^2 + y^2 + z^2)}{r^2} \frac{\partial^2 \rho}{\partial r^2} \quad (2.46)$$

$$= \frac{2}{r} \frac{\partial \rho}{\partial r} + \frac{\partial^2 \rho}{\partial r^2} = \frac{1}{r} \frac{\partial^2}{\partial r^2} (r\rho) \quad (2.47)$$

The wave equation then becomes

$$\frac{1}{r} \frac{\partial^2}{\partial r^2} [r\rho(r,t)] - \frac{1}{c^2} \frac{\partial^2}{\partial t^2} \rho(r,t) = 0 \quad (2.48)$$

or

$$\frac{\partial^2}{\partial r^2}[r\rho(r,t)] - \frac{1}{c^2} \frac{\partial^2}{\partial t^2}[r\rho(r,t)] = 0 \quad (2.49)$$

Because the mathematical interpretation of the differential equation for the function $[r\rho(r,t)]$ is same as the one-dimensional wave equation, general solution for this expression can be written in the form of equation (2.1) as

$$r\rho(r,t) = f\left(t - \frac{r}{c}\right) + g\left(t + \frac{r}{c}\right) \quad (2.50)$$

The actual disturbance ρ then takes the form

$$\rho(r,t) = \frac{1}{r} f\left(t - \frac{r}{c}\right) + \frac{1}{r} g\left(t + \frac{r}{c}\right) \quad (2.51)$$

The first term in equation (2.51) can be interpreted as spherically symmetric disturbance that originates at the origin and propagates outward with the velocity c . The amplitude of the disturbance falls off as $1/r$ [7].

CHAPTER 3

HUYGENS – FRESNEL AND FIELD INTEGRAL

3.1 Introduction

In this chapter the theoretical and mathematical background that is used in the simulation is given. The mainly used mathematical term in the simulation is Huygens-Fresnel principle. Extended form of the Huygens-Fresnel definition of field integral is used to find the field of the propagating light. By using this field, the intensity of the light beam can be derived. The light beam has a spatial random source phase which is described in this chapter. Parameters of atmospheric turbulence affecting the propagating light are also given.

3.2 The Huygens - Fresnel Principle

The Huygens-Fresnel principle states that every point on the primary wavefront can be thought as a continuous emitter of secondary wavelets (sources) and these secondary wavelets combine to produce a new wavefront in the direction propagation.

The basic idea of the Huygens-Fresnel principle is that the light disturbance at a point arises from the superposition of secondary waves that proceed from a surface situated between this point and the light source. This principle expresses the solution of the homogeneous wave equation, at an arbitrary point in the field, in

terms of the solution and its first derivatives at all points on an arbitrary closed surface surrounding the point [6].

The laser shows the property of a monochromatic wave having a well-defined frequency ν . We can calculate the irradiance at a given point by taking the square of component of field at this frequency. The Fourier integral of the field on a fixed point \mathbf{r} is

$$E(\mathbf{r}, t) = \int_{-\infty}^{\infty} \hat{E}(\mathbf{r}, \nu) e^{2\pi i \nu t} d\nu \quad (3.1)$$

The Fourier coefficient $\hat{E}(\mathbf{r}, \nu)$ still depends on the position. Because the original field $E(\mathbf{r}, t)$ is real, \hat{E} must obey the condition

$$\hat{E}(\mathbf{r}, \nu)^* = \hat{E}(\mathbf{r}, -\nu) \quad (3.2)$$

If we write

$$\hat{E}(\mathbf{r}, \nu) = \left| \hat{E}(\mathbf{r}, \nu) \right| e^{i\phi(\mathbf{r}, \nu)} \quad (3.3)$$

we can evaluate the solution

$$E(\mathbf{r}, t) = 2 \int_0^{\infty} \left| \hat{E}(\mathbf{r}, \nu) \right| \cos[2\pi\nu t + \phi(\mathbf{r}, \nu)] d\nu \quad (3.4)$$

$$= \text{Re} \int_0^{\infty} 2 \hat{E}(\mathbf{r}, \nu) e^{2\pi i \nu t} d\nu \quad (3.5)$$

Equation (3.4) expresses the field at \mathbf{r} as the real part of a superposition of complex exponentials with positive frequency ν and with spatially dependent complex coefficient $2\hat{E}(\mathbf{r}, \nu)$ [7].

If we write $E(\mathbf{r}, t)$ in terms of a complex spatially dependent, time-independent wave function $\tilde{E}(\mathbf{r})$, it becomes

$$E(\mathbf{r}, t) = \text{Re} 2 \hat{E}(\mathbf{r}, \nu) e^{2\pi i \nu t} \equiv \text{Re} \tilde{E}(\mathbf{r}) e^{2\pi i \nu t} \quad (3.6)$$

If equation (3.5) is substituted into the time-independent three-dimensional wave equation, given by,

$$\nabla^2 \tilde{E} - \frac{1}{c^2} \frac{\partial^2 E}{\partial t^2} = 0 \quad (3.7)$$

time-independent wave equation which is also known as Helmholtz equation is derived as

$$\nabla^2 \tilde{E} + k^2 \tilde{E} = 0 \quad (3.8)$$

where $k = 2\pi\nu / c = 2\pi / \lambda$.

If we consider a plane wave propagating in the $+x$ direction:

$$E(\mathbf{r}, t) = A \cos \left[2\pi\nu \left(t - \frac{x}{c} \right) + \phi \right] = \quad (3.9)$$

$$= \text{Re} \left[\left(A e^{i\phi} e^{-ikx} \right) e^{2\pi i\nu t} \right] \quad (3.10)$$

It can be found that equation (3.8) obeys equation (3.7) by identifying the factors in parenthesis $E(\mathbf{r})$.

$$\tilde{E} = A e^{i\phi} e^{-ikx} \quad (3.11)$$

where $A e^{i\phi}$ is a complex constant. And similarly an exponential of the form

$$\tilde{E} = A e^{i\phi} e^{-i\mathbf{k}\cdot\mathbf{r}} \quad (3.12)$$

is a solution of equation (3.12) that represents the spatial part of a plane wave propagating in the direction of the vector \mathbf{k} , where

$$|\mathbf{k}| = k = \frac{2\pi}{\lambda} \quad (3.13)$$

The time-dependent counter part is

$$E(\mathbf{r}, t) = A \cos(2\pi\nu t - \mathbf{k} \cdot \mathbf{r} + \phi) \quad (3.14)$$

A time-independent spherical wave propagating outward from a point source can be written

$$E(\mathbf{r}, t) = \frac{A}{\rho} \cos[2\pi\nu t - k\rho + \phi] \quad (3.15)$$

where \mathbf{r}_s is the center of the wave and $\rho = |\mathbf{r} - \mathbf{r}_s|$ is its radius. This can be written as the real part of

$$E(\mathbf{r}, t) = \left(A e^{i\phi} \frac{e^{-ik\rho}}{\rho} \right) e^{2\pi i\nu t} \quad (3.16)$$

The effects of interference by superposition of spherical waves required the superposition of a limited number of these elementary plane and spherical waves. Adding two spherical waves

$$\tilde{E}(\mathbf{r}) = \frac{A_1}{|\mathbf{r} - \mathbf{r}_1|} e^{-k|\mathbf{r} - \mathbf{r}_1|} + \frac{A_2}{|\mathbf{r} - \mathbf{r}_2|} e^{-k|\mathbf{r} - \mathbf{r}_2|} \quad (3.17)$$

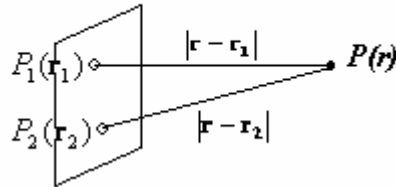


Figure 3-1: Diffraction by two pinholes in a screen.

In figure 3-1, the pinholes are so small that each radiates a single Huygens' wavelet. From P_1 the wave P is of the form $\frac{A_1}{|\mathbf{r} - \mathbf{r}_1|} e^{-ik|\mathbf{r} - \mathbf{r}_1|}$. The complex coefficient A_1 determines the strength and phase of the wavelet. According to Huygens' Principle, this wavelet is reradiated by incident wave P_1 impinging on the screen from the left. Thus, it can be expected A_1 to be proportional to the incident field $\tilde{E}_{inc}(\mathbf{r}_1)$, also A_1 to be proportional to $\Delta\sigma_1$, the element area of the pinhole, provided that it is so small that $\tilde{E}_{inc}(\mathbf{r}')$ and $k|\mathbf{r} - \mathbf{r}'|$ can be treated as constant for \mathbf{r}' anywhere in the pin hole [7]. So

$$A_1 = C \tilde{E}_{inc}(\mathbf{r}_1) \Delta\sigma_1 \quad (3.18)$$

The factor C in equation (3.18) is defined as

$$C = \frac{ik}{2\pi} = \frac{i}{\lambda} \quad (3.19)$$

Thus, equation (3.18) can be written as

$$A_1 \approx \frac{i}{\lambda} \tilde{E}_{inc}(\mathbf{r}_1) \Delta\sigma_1 \quad (3.20)$$

Similarly from the other pinhole

$$A_2 \approx \frac{i}{\lambda} \tilde{E}_{inc}(\mathbf{r}_2) \Delta\sigma_2 \quad (3.21)$$

Therefore the spatial part of the field at point P is given by

$$\tilde{E}(\mathbf{r}) = \frac{i}{\lambda} \left[\frac{\tilde{E}_{inc}(\mathbf{r}_1)}{|\mathbf{r} - \mathbf{r}_1|} e^{-ik|\mathbf{r} - \mathbf{r}_1|} \Delta\sigma_1 + \frac{\tilde{E}_{inc}(\mathbf{r}_2)}{|\mathbf{r} - \mathbf{r}_2|} e^{-ik|\mathbf{r} - \mathbf{r}_2|} \Delta\sigma_2 \right] \quad (3.22)$$

For N pinholes at \mathbf{r}_j , $j = 1, 2, \dots, N$ with areas $\Delta\sigma_j$ equation (3.22) can be generalized to

$$\tilde{E}(\mathbf{r}) = \frac{i}{\lambda} \sum_{j=1}^N \frac{\tilde{E}_{inc}(\mathbf{r}_j)}{|\mathbf{r} - \mathbf{r}_j|} e^{-ik|\mathbf{r} - \mathbf{r}_j|} \Delta\sigma_j \quad (3.23)$$

Equation (3.23) is a good approximation to the total field at P . In the limit as all the $\Delta\sigma$'s tend to zero, it is obtained the surface integral

$$\tilde{E}(\mathbf{r}) = \frac{i}{\lambda} \iint_{\Sigma_0} \tilde{E}_{inc}(\mathbf{r}') \frac{e^{-ik|\mathbf{r} - \mathbf{r}'|}}{|\mathbf{r} - \mathbf{r}'|} d\sigma \quad (3.24)$$

Where $d\sigma$ represents an infinitesimal element of surface area at the point \mathbf{r}' which is a general point in the opening Σ_0 .

Extended Huygens-Fresnel

The aperture is in the plane through the origin \mathbf{O} normal to the z axis. Here

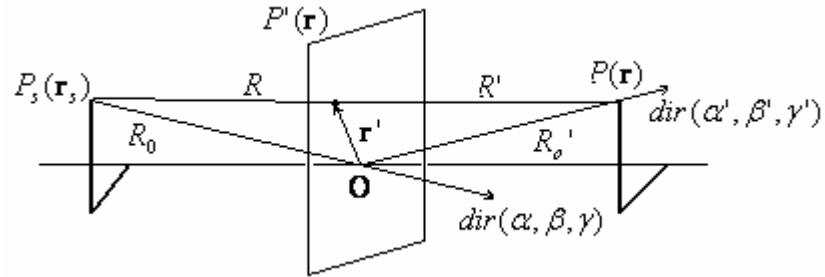


Figure 3-2: Spherical wave propagation.

P' with position vector $\mathbf{r}' = (x', y', 0)$ is a typical point in the aperture. The point source of monochromatic light is at P_s with position vector \mathbf{r}_s . The observation point is at $P(\mathbf{r})$. In equation (3.24), $|\mathbf{r}' - \mathbf{r}_s| = R$ and $|\mathbf{r} - \mathbf{r}'| = R'$ then it can be written as

$$\tilde{E}(\mathbf{r}) = \frac{i}{\lambda} A \iint_{\Sigma_0} \frac{e^{-ik(R'+R)}}{RR'} d\sigma \quad (3.25)$$

where A is the amplitude of the incident wave at unit distance from P_s .

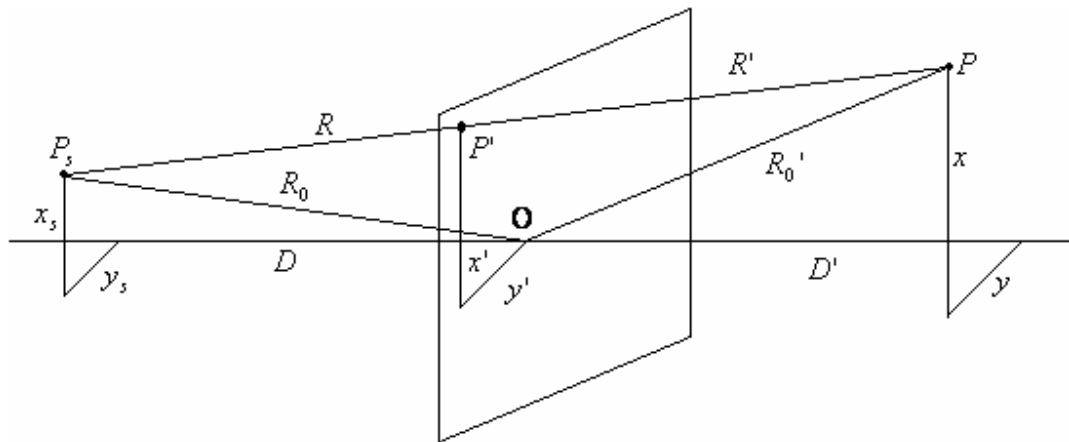


Figure 3-3: Derivation of Huygens-Fresnel diffraction integrals.

Figure 3-3 defines the geometry. The starting equation is (3.25).

For Fraunhofer diffraction we expanded R about R_0 and R' about R'_0 and obtained for R

$$R = R_0 + \alpha x' + \beta y' + \frac{1}{2} \left[\frac{x'^2 + y'^2 + (\alpha x' + \beta y')^2}{R_0} \right] + \dots \quad (3.26)$$

In order to keep last term small, Fraunhofer approximation is made $|x'| \ll \sqrt{R_0 \lambda}$, $|y'| \ll \sqrt{R_0 \lambda}$, but α and β is not assumed to be small.

The quadratic term in the above expansion about R_0 is lengthy because of the presence of $x'y'$ cross term obtained by multiplying out

$$\frac{(\alpha x' + \beta y')^2}{2R_0} \quad (3.27)$$

This can be eliminated only by assuming that α and β are small. When this is done, it should be also expanded R_0 about D . This is equivalent to treating x_s , x_s , x' and y' on an equal footing and expanding R about D . Thus,

$$R = \sqrt{D^2 + (x_s - x')^2 + (y_s - y')^2} = D \left[1 + \frac{(x_s - x')^2}{D^2} + \frac{(y_s - y')^2}{D^2} \right]^{1/2} \quad (3.28)$$

and expand to obtain

$$R = D + \frac{(x_s - x')^2}{2D} + \frac{(y_s - y')^2}{2D} - \frac{1}{8} \frac{[(x_s - x')^2 + (y_s - y')^2]^2}{D^3} + \dots \quad (3.29)$$

It is intended to drop the last term in equation (3.21). It must be much less than λ , and almost always is in the cases of interest.

Similarly we obtain the result

$$\begin{aligned} R' &= \sqrt{D'^2 + (x_s - x')^2 + (y_s - y')^2} \\ &= D' + \frac{(x - x')^2}{2D'} + \frac{(y - y')^2}{2D'} - \frac{1}{8} \frac{[(x - x')^2 + (y - y')^2]^2}{D'^3} + \dots \end{aligned} \quad (3.30)$$

In the denominator of equation (3.20) it is replaced R, R' by D, D' since the denominators are slowly varying. The exponential varies much more rapidly, and more care is required. In the exponent we shall put

$$\begin{aligned} |P_s P' P| &= R + R' = D + D' + \left[\frac{(x - x')^2}{2D'} + \frac{(x_s - x')^2}{2D} \right] \\ &\quad + \left[\frac{(y - y')^2}{2D'} + \frac{(y_s - y')^2}{2D} \right] \end{aligned} \quad (3.31)$$

The integral equation (3.25) can be reduced to standard form by completing the squares in equation (3.31).

$$[\dots]_x \equiv \left[\frac{(x - x')^2}{2D'} + \frac{(x_s - x')^2}{2D} \right] = \frac{x^2}{2D'} + \frac{x_s^2}{2D} + \frac{x'^2}{2} \left(\frac{1}{D} + \frac{1}{D'} \right) - x' \left(\frac{x}{D'} + \frac{x_s}{D} \right) \quad (3.32)$$

The coefficient ($-x'$) is

$$\frac{x}{D'} + \frac{x_s}{D} = \frac{Dx + D'x_s}{DD} = \left(\frac{Dx + D'x_s}{D + D'} \right) \left(\frac{D + D'}{DD'} \right) \quad (3.33)$$

We define two new variables

$$\rho = \frac{DD'}{D + D'}, \quad \frac{1}{\rho} = \frac{D + D'}{DD'} = \frac{1}{D} + \frac{1}{D'} \quad (3.34)$$

and

$$x_m = \frac{Dx + D'x_s}{D + D'} \quad (3.35)$$

Then the coefficient of ($-x'$) is x_m / ρ . The coefficient of x'^2 is

$$\frac{1}{2} \left(\frac{1}{D} + \frac{1}{D'} \right) = \frac{1}{2\rho} \quad (3.36)$$

Thus

$$\begin{aligned} [\dots]_x &= \frac{x^2}{2D'} + \frac{x_s^2}{2D} + \frac{x'^2}{2\rho} - \frac{x'x_m}{\rho} = \frac{x^2}{2D'} + \frac{x_s^2}{2D} \\ &+ \frac{1}{2\rho} (x'^2 - 2x'x_m + x_m^2) - \frac{x_m^2}{2\rho} \end{aligned} \quad (3.37)$$

$$= \frac{(x' - x_m)^2}{2\rho} + \frac{Dx^2 + D'x_s^2 - (Dx + D'x_s)^2 / (D + D')}{2DD'} \quad (3.38)$$

$$= \frac{(x' - x_m)^2}{2\rho} + \frac{(x - x_s)^2}{2(D + D')} \quad (3.39)$$

Similarly, if we define

$$y_m = \frac{Dy + D'y_s}{D + D'} \quad (3.40)$$

Algebraic manipulations lead to

$$[\dots]_y = \left[\frac{(y - y')^2}{2D'} + \frac{(y_s - y')^2}{2D} \right] = \frac{(y' - y_m)^2}{2\rho} + \frac{(y - y_s)^2}{2(D + D')} \quad (3.41)$$

Equations (3.37, 41), when inserted into equation (3.25), give

$$|P_s P' P| = R + R' = \left[D + D' \frac{(x - x_s)^2 + (y - y_s)^2}{2(D + D')} \right] + \left[\frac{(x' - x_m)^2 + (y' - y_m)^2}{2\rho} \right] \quad (3.42)$$

The first bracketed term in equation (3.42) is a good approximation to the distance from P_s to P :

$$|P_s P| = \sqrt{(D + D')^2 + (x - x_s)^2 + (y - y_s)^2} \quad (3.43)$$

$$= (D + D') \left[1 + \frac{(x - x_s)^2 + (y - y_s)^2}{(D + D')^2} \right]^{1/2} \quad (3.44)$$

$$= (D + D') + \frac{(x - x_s)^2 + (y - y_s)^2}{2(D + D')} \quad (3.45)$$

Then equation (3.42) can be written

$$|P_s P' P| = |P_s P| + \left[\frac{(x' - x_m)^2 + (y' - y_m)^2}{2\rho} \right] \quad (3.46)$$

and equation (3.20) becomes [7]

$$\tilde{E}(\mathbf{r}) = \frac{iA}{\lambda DD'} e^{-ik|P_s P|} \iint_{\Sigma_0} \exp \left\{ -\frac{ik}{2\rho} [(x' - x_m)^2 + (y' - y_m)^2] \right\} dx' dy' \quad (3.47)$$

One further change is made with the use of equation (3.24)

$$\frac{1}{DD'} = \frac{(D + D')}{DD'} \frac{1}{(D + D')} = \frac{1}{(D + D')\rho} \approx \frac{1}{|P_s P|\rho} \quad (3.48)$$

Then the factor in front of the integral becomes

$$\frac{iA}{\lambda DD'} e^{-ik|P_s P|} = \frac{i}{\lambda\rho} \frac{A e^{-ik|P_s P|}}{|P_s P|} = \frac{i}{\lambda\rho} \tilde{E}_{na}(\mathbf{r}) \quad (3.49)$$

where

$$\tilde{E}_{na}(\mathbf{r}) = \frac{Ae^{-ik|P_s P|}}{|P_s P|} \quad (3.50)$$

is the field that would be observed $P(\mathbf{r})$ if there were no aperture at all. The Huygens-Fresnel field integral under this approximation and with the inclusion of the complex amplitude term due to atmospheric turbulence becomes

$$\tilde{E}(\mathbf{r}) = \frac{i}{\lambda\rho} \tilde{E}_{na}(\mathbf{r}) \iint_{\Sigma_0} \exp\left\{-\frac{i\pi}{\lambda\rho}[(x'-x_m)^2 + (y'-y_m)^2] + \psi_t\right\} dx' dy' \quad (3.51)$$

where λ is the wavelength, ψ_t represents the random part of the complex phase of a spherical wave propagating from the source point to the receiver point. This form of the propagation integral given by equation (3.51) is known as the extended Huygens-Fresnel principle.

3.3 Laser Intensity

Intensity is found by multiplying the field with its complex conjugate. In free space, it is formulated by the extended Huygens-Fresnel formula in equation (3.51) when ψ_t is taken as 0.

In equation (3.51), it is assumed that the amplitude of the field integral $\tilde{E}_{na}(\mathbf{r})=A=1$. This gives us a square aperture laser source. Also in same equation ρ denotes the length and direction of propagation. The direction of propagation is

z so it can be defined as $z = \rho$. The source of the laser is square so the integration is taken over the source aperture (surface) S . The parameters can be changed as

$$\begin{aligned}
 u(x, y, z) &= \tilde{E}(\mathbf{r}) \\
 x &= x_m \\
 y &= y_m \\
 x_0 &= x' \\
 y_0 &= y' \\
 z &= \rho
 \end{aligned}
 \quad \text{Transformations}$$

By using these changes field integral becomes

$$u(x, y, z) = \frac{k}{2\pi i z} A \iint_S \exp\left\{-\frac{ik}{2z}(x-x_0)^2\right\} \exp\left\{-\frac{ik}{2z}(y-y_0)^2\right\} dx_0 dy_0 \quad (2.52)$$

The intensity of a given coordinate (x, y, z) is evaluated by the multiplication of field integral with its complex conjugate [8].

$$\langle I(x, y, z) \rangle = \langle u(x, y, z) u^*(x, y, z) \rangle \quad (3.53)$$

where $u^*(x, y, z)$ is the complex conjugate of field integral. The detailed form of intensity in free space (in the absence of turbulence) is

$$\begin{aligned}
\langle I(x, y, z) \rangle &= \left(\frac{k A}{2 \pi z} \right)^2 \iint_s \exp \left\{ -\frac{i k}{2 z} (x - x_o)^2 \right\} \exp \left\{ -\frac{i k}{2 z} (y - y_o)^2 \right\} dx_o dy_o \\
&\times \iint_s \exp \left\{ \frac{i k}{2 z} (x - x_o)^2 \right\} \exp \left\{ \frac{i k}{2 z} (y - y_o)^2 \right\} dx_o dy_o
\end{aligned} \tag{3.54}$$

3.4 Spatial Random Source Phase

The parameter $\psi(x_o, y_o)$ denoting the spatial random complex phase of a spherical wave propagating in free space from point P_s to P is, the field integral in equation (3.52) becomes

$$u(x, y, z) = \frac{k}{2 \pi i z} A \iint_s \exp \left\{ -\frac{i k}{2 z} (x - x_o)^2 \right\} \exp \left\{ -\frac{i k}{2 z} (y - y_o)^2 \right\} \exp \{ \psi(x_o, y_o) \} dx_o dy_o \tag{3.55}$$

The phase ψ is taken as random which is uniformly distributed.[9,10] The probability density function $f(x)$ is shown in figure 3-4. In the simulation, the given distribution is expanded with **expansion coefficients** from 0-to- 2π by multiplying $f(x)$ with the coefficients. The distribution is taken over $[-0.5, 0.5]$ because the maximum expansion coefficient is 2π . This expansion causes an increase in the magnitude of the spatial random source phase. Greater the expansion coefficient, greater the magnitude of the phase. The effects of this increase in the magnitude of the phase on the profile of the intensity of the laser from 0-to- 2π are investigated both in speckle and atmospheric turbulence cases.

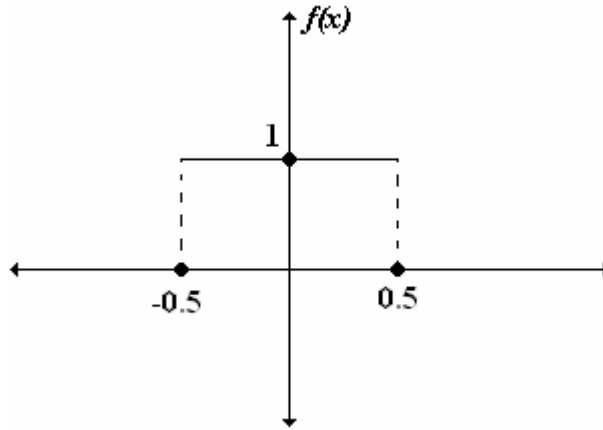


Figure 3-4: Probability Density Function of spatial random source phase.

In order to make sure the coordinate dependency of the phase ψ , each element on phase matrix is multiplied with the sum of coordinates x_0, y_0 .

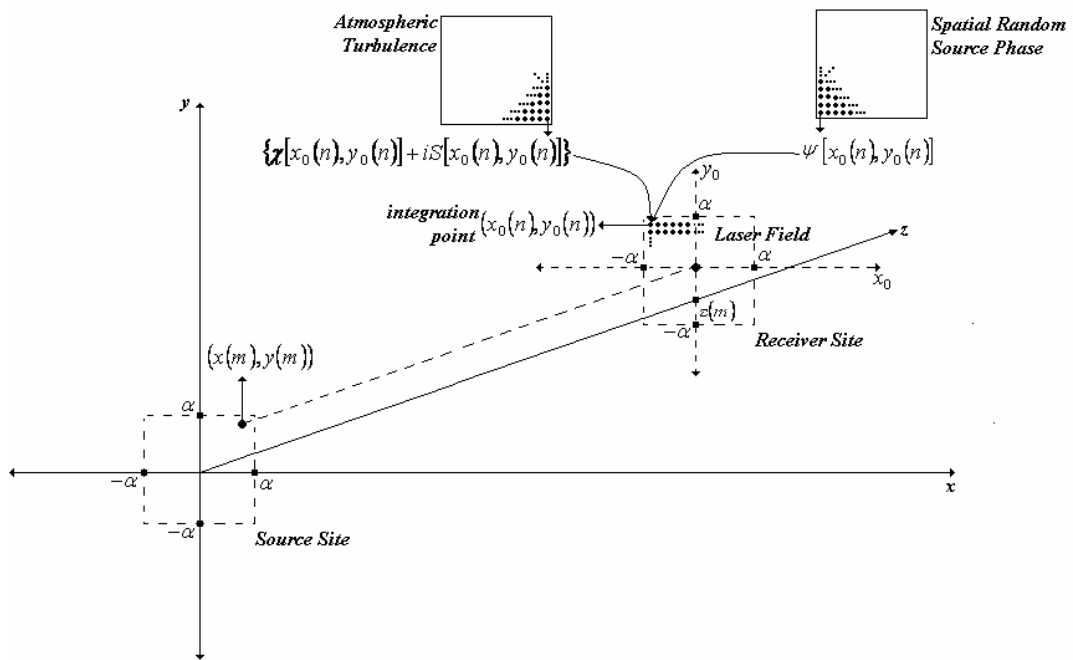


Figure 3-5: Propagation of field on x_0, y_0 plane and integration point on field.

Coordinate dependent elements of spatial random source phase is included in calculation in every integration point on the field integral dependent to x_0, y_0 . As it can be seen from the figure 3-5 on each integration point of the field integral taken on x_0, y_0 plane at receiver site in order to evaluate the intensity value of a given point $(x(m), y(m))$, both a value from spatial random source phase and atmospheric turbulence (which will be mentioned in detail in section 3.5) planes are included into the integration. This means, during integration of the field $u(x, y, z)$ on each value of x_0, y_0 , the spatial random source phase $\psi(x_0, y_0)$ takes different complex random values having uniform distribution [11].

By using the intensity formula (3.53), the intensity value in free space for (x_m, y_m) and the propagation distance $z = z_m$ can be found in detail as

$$\begin{aligned} \langle I(x, y, z) \rangle = & \left(\frac{k A}{2 \pi z} \right)^2 \iint_S \exp \left\{ -\frac{i k}{2 z} (x - x_o)^2 \right\} \exp \left\{ -\frac{i k}{2 z} (y - y_o)^2 \right\} \exp \{ \psi(x_o, y_o) \} dx_o dy_o \\ & \cdot \iint_S \exp \left\{ \frac{i k}{2 z} (x - x_o)^2 \right\} \exp \left\{ \frac{i k}{2 z} (y - y_o)^2 \right\} \exp \{ \psi^*(x_o, y_o) \} dx_o dy_o \end{aligned} \quad (3.56)$$

where $\psi^*(x_0, y_0)$ is the complex conjugate of spatial random source phase.

3.5 Parameters of Atmospheric Turbulence

The parameters $[\chi(x_0, y_0, z) + iS(x_0, y_0, z)]$ denoting the atmospheric turbulence of a turbulent medium through which the wave is propagating, the field integral in equation (3.55) becomes

$$u(x, y, z) = \frac{k}{2\pi i z} A \iint_s \exp\left\{-\frac{ik}{2z}(x-x_o)^2\right\} \exp\left\{-\frac{ik}{2z}(y-y_o)^2\right\} \exp\{\psi(x_o, y_o)\} \exp\{[\chi(x_o, y_o, z) + iS(x_o, y_o, z)]\} dx_o dy_o \quad (3.57)$$

Here $S(x_o, y_o, z)$ is the random phase introduced due to atmospheric turbulence. The real part of the atmospheric turbulence complex amplitude, $\chi(x_o, y_o, z)$, i.e., log-amplitude fluctuations, is a Gaussian distributed random value having zero mean. The variance of the log-amplitude fluctuations (σ_χ^2) is given in [12,13]

$$\sigma_\chi^2 = 0.123 C_n^2 z^{11/6} k^{7/6} \quad (3.58)$$

where C_n^2 is the structure constant of refractive index fluctuations of the turbulence, z is the propagation path length and k is the wave number and equals to $2\pi/\lambda$, λ being the wavelength.

If the source size is small we could make the assumption that $\sigma_\chi^2 \ll 0.25$. Because $\sigma_\chi^2 \ll 0.25$ it can be assumed as $\sigma_\chi^2 < 0.025$ and the maximum variance of parameter (σ_χ^2) can be derived from

$$\sigma_{\chi_{\max}}^2 = (0.025 \cdot 0.123) C_n^2 z^{11/6} k^{7/6} \quad (3.59)$$

The imaginary part of the atmospheric turbulence, i.e., $S(x_o, y_o, z)$ is also Gaussian distributed over the interval $[-\pi, \pi]$, the mean being zero.

Atmospheric turbulence is included in the field integral, same as with the spatial random source phase, on every integration point of field integral x_0, y_0 , as seen in figure 3-5, coordinate dependent values $\chi(x_0, y_0, z), S(x_0, y_0, z)$ take different values according to their disturbance properties on each x_0, y_0 value. The intensity value on (x_m, y_m) can be derived in detail as

$$\begin{aligned}
\langle I(x_m, y_m, z_m) \rangle = & \left(\frac{k A}{2 \pi z} \right)^2 \iint_S \exp \left\{ -\frac{i k}{2 z} (x - x_o)^2 \right\} \exp \left\{ -\frac{i k}{2 z} (y - y_o)^2 \right\} \\
& \cdot \exp \{ \psi(x_0, y_0) \} \exp \{ [\chi(x_0, y_0, z) + i S(x_0, y_0, z)] \} dx_0 dy_0 \\
& \cdot \iint_S \exp \left\{ \frac{i k}{2 z} (x - x_o)^2 \right\} \exp \left\{ \frac{i k}{2 z} (y - y_o)^2 \right\} \\
& \cdot \exp \{ \psi^*(x_0, y_0) \} \exp \{ [\chi(x_0, y_0, z) - i S(x_0, y_0, z)] \} dx_0 dy_0
\end{aligned} \tag{3.60}$$

CHAPTER 4

SIMULATION

4.1 Introduction

This chapter involves the numerical methods for simulating the field integral discussed in chapter 3. In order to evaluate the field integral, first the Gaussian-numerical integration method will be introduced. The field integral will be evaluated for three cases, first with no source phase in vacuum, second with source phase in vacuum and third with source phase and in atmospheric turbulence. At the end, the results of the simulations and comparative graphics are given.

4.2 Numerical Integration of Field Integral

In order to numerically evaluate the field integral of the propagating light through spatial medium, Gaussian quadratures is used as the numerical integration method.

In classical methods, the integral of a function is evaluated by the sum of its functional values at a set of equally spaced points, multiplied by the chosen weighting coefficients or step sizes. The main difference of Gaussian quadratures is to give the evaluation process the freedom choosing not only the weighting coefficients, but also the location of the functional values at which the function is

to be evaluated. So the functional values are not equally spaced. Another additional feature of Gaussian quadrature formulas is that the choice of weights and functional values can be arranged in order to make the integral exact for a class of integrands “polynomials times some known function $W(x)$ ”. The function $W(x)$ can be chosen to remove singularities. Given $W(x)$ and given integer N , a set of weights w_j and functional values x_j can be found such that [14]

$$\int_a^b W(x)f(x)dx \approx \sum_{j=1}^N w_j f(x_j) \quad (4.1)$$

The integration formula in (4.1) can also be written with the weight function $W(x)$ $g(x) \equiv w(x)f(x)$ and $v_j \equiv w_j / W(x_j)$. Then equation (4.1) becomes

$$\int_a^b g(x)dx \approx \sum_{j=1}^N v_j g(x_j) \quad (4.2)$$

A set of polynomials can be found that it includes exactly one polynomial of order j , called $p_j(x)$, for each $j = 0,1,2,\dots$, and all of which are orthogonal over the specified weight function $W(x)$. A set of constructive procedure for finding such a set is the recurrence relation

$$\begin{aligned} p_{-1}(x) &\equiv 0 \\ p_0(x) &\equiv 1 \\ p_{j+1}(x) &= (x - a_j)p_j(x) - b_j p_{j-1}(x) \quad j = 0,1,2,\dots \end{aligned} \quad (4.3)$$

The functional values of the N-point Gaussian quadrature formulas (4.1) and (4.2) with weight function $W(x)$ in the interval (a,b) are the roots of the orthogonal polynomial $p_N(x)$ for the same interval and weighting function. This is the fundamental theorem of the Gaussian quadratures, and allows finding the functional values for any particular case.

Once the functional values x_1, \dots, x_N are known, w_j for $j = 1, \dots, N$ can be found by [15]

$$\begin{bmatrix} p_0(x_1) & \cdots & p_0(x_N) \\ p_1(x_1) & \cdots & p_1(x_N) \\ \vdots & & \vdots \\ p_{N-1}(x_1) & \cdots & p_{N-1}(x_N) \end{bmatrix} \begin{bmatrix} w_1 \\ w_2 \\ \vdots \\ w_N \end{bmatrix} = \begin{bmatrix} \int_a^b W(x) p_0(x) dx \\ 0 \\ \vdots \\ 0 \end{bmatrix} \quad (4.4)$$

The field integral can be defined for Gaussian quadratures as

$$u(x, y, z) = \sum_{x_0=-\alpha}^{\alpha} \sum_{y_0=-\alpha}^{\alpha} \left[\frac{Ak}{2\pi i z} \exp\left\{-\frac{ik}{2z}(y-y_0)^2\right\} \exp\left\{-\frac{ik}{2z}(x-x_0)^2\right\} w_{x_0} w_{y_0} \right] \quad (4.5)$$

If spatial random source phase and atmospheric turbulence are introduced, numerical field integration can be done by

$$u(x, y, z) = \sum_{x_0=-\alpha}^{\alpha} \sum_{y_0=-\alpha}^{\alpha} \frac{Ak}{2\pi i z} \exp\left\{-\frac{ik}{2z}(y-y_0)^2\right\} \exp\left\{-\frac{ik}{2z}(x-x_0)^2\right\} \exp\{\psi(x_0, y_0)\} \exp\{\chi(x_0, y_0, z) + iS(x_0, y_0, z)\} w_{x_0} w_{y_0} \quad (4.6)$$

4.3 Simulation Results

Intensity profile analysis of Free Space Optics systems using 1550 nm laser is evaluated for three different approaches. In the first approach, random source phase and atmospheric turbulence are not included in the simulation. For this condition, intensity profile of laser is evaluated for propagation distances of 2km and 5km. In the second approach, random source phase is included to simulation with the given PDF in figure 3-4 and the expansion coefficients discussed in section 3-4 is increased from 0-to- 2π and this process is repeated for various propagation distances up to 5 km. In the third case, both the random source phase and atmospheric turbulence are included in the simulation and for various propagation distances; the behavior of the source phase is same as in the second approach. The Matlab code for these approaches is given in the appendix A to E.

In figures 4-1 and 4-2 both the effects of spatial random source phase and atmospheric turbulence are neglected and their parameters are not included in the field integral. The field integral is evaluated for propagation distances of 2000m and 5000m. In figure 4-3, beam spread at the receiver plane is plotted. As seen from the figures 4-1, 4-2 and 4-3, the beam spread increases as the propagation distance increases. Figure 4-3 shows that the increase in propagation distance has an increasing effect on the beam spread, but the shape of the intensity profile is not affected from the propagation distance so that the beam keeps its shape.

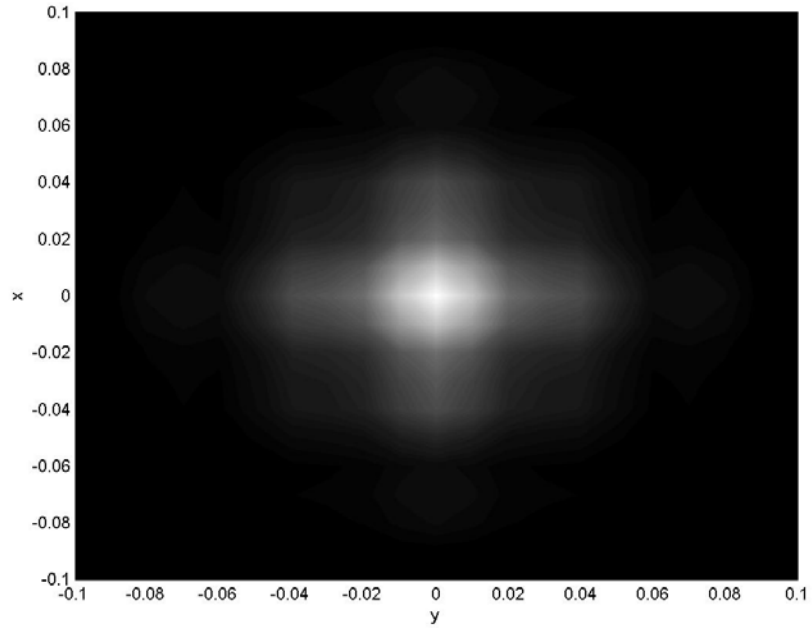


Figure 4-1 : Laser intensity profile of FSO system using 1550nm wavelength laser for a 2000m propagation distance. Random source phase and atmospheric turbulence are not included.

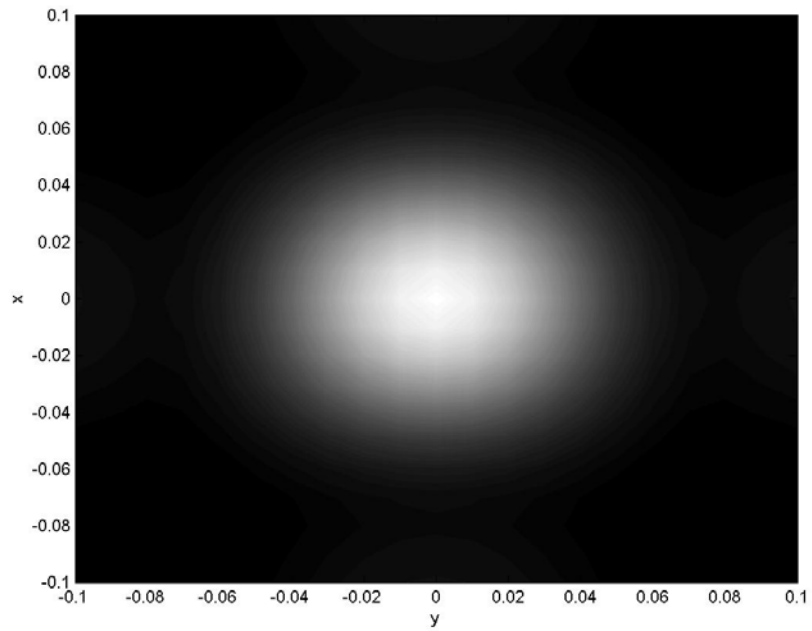


Figure 4-2 : Laser Intensity profile of FSO system using 1550nm wavelength laser for a 5000m propagation distance. Random source phase and atmospheric turbulence are not included.

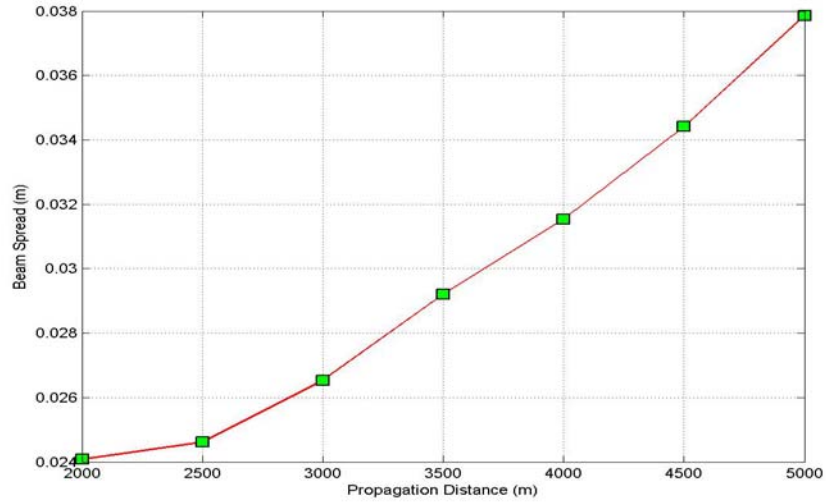


Figure 4-3 : Laser beam spread of FSO system using 1550nm wavelength laser due to propagation distance. Random source phase and atmospheric turbulence are not included.

In figures 4-4 to 4-9 spatial random phase is included in the field integral by increasing the expansion coefficient for each evaluation of the integral. This process is repeated for each propagation distance used in the previous case. In this case it can be seen from the figures that the beam spread has an increasing behavior. Besides, during evaluation process for each propagation distance the expansion coefficient (discussed in section 3.4) of the spatial random source phase is increased from 0-to- 2π . This has an effect both on the beam spread and the intensity profile. The bigger the expansion coefficient of the spatial random source phase, the larger is the beam spread for that propagation distance, which is seen in figure 4-10. As seen in the figures 4-4 to 4-9 the intensity profile loses its shape. The reason for the rugby-ball shape is the coordinate dependence of the phase ψ , i.e., multiplying the sum of coordinates by the phase values. At larger expansion coefficient values or magnitudes of the source phase, detection process may be adversely affected at the receiver site and this will degrade the performance of the FSO system.

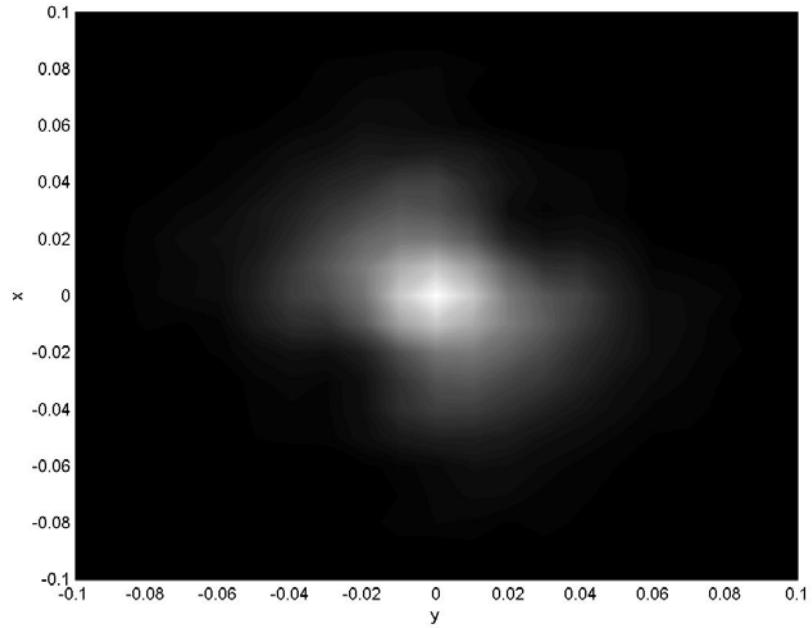


Figure 4-4 : Laser Intensity profile of FSO system using 1550nm wavelength laser for a 2000m propagation distance. Random source phase included and expansion coefficient is π .

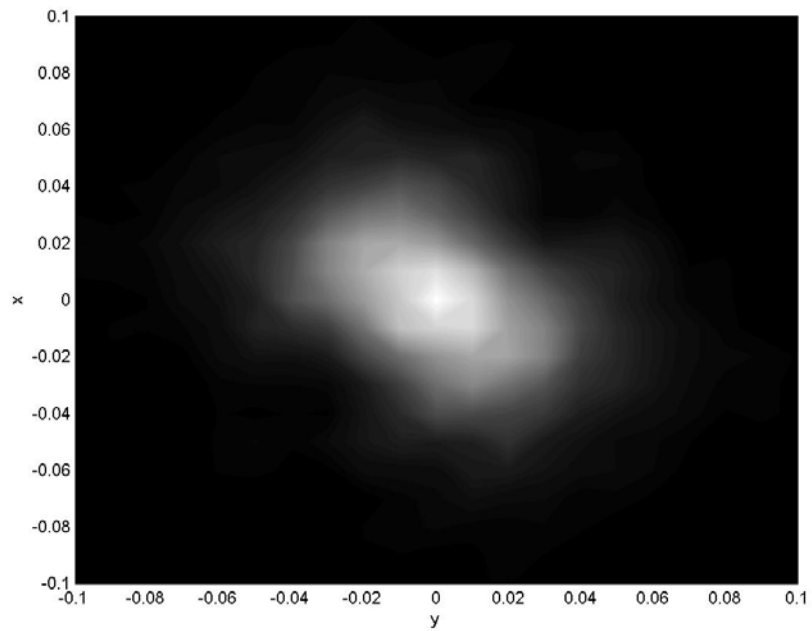


Figure 4-5 : Laser Intensity profile of FSO system using 1550nm wavelength laser for a 2000m propagation distance. Random source phase included and expansion coefficient is 2π .

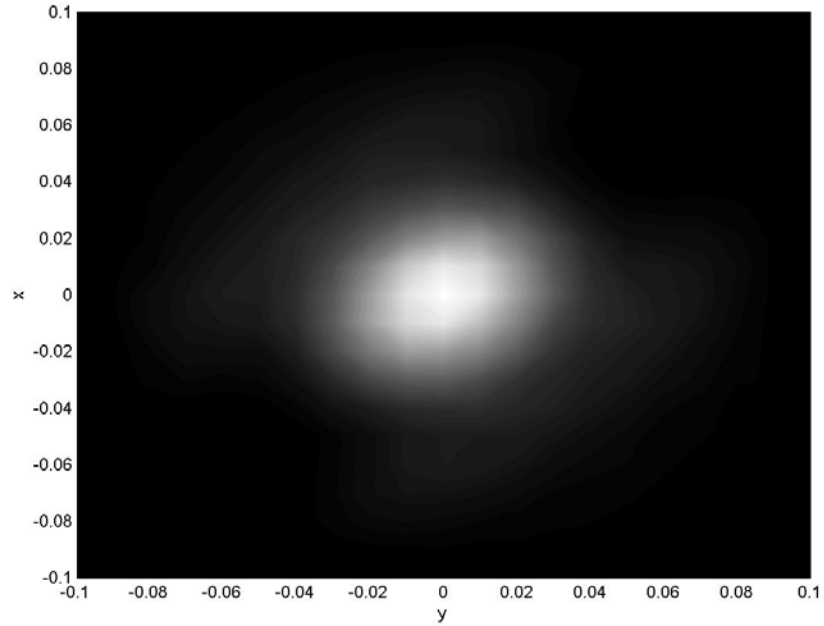


Figure 4-6 : Laser Intensity profile of FSO system using 1550nm wavelength laser for a 3000m propagation distance. Random source phase included and expansion coefficient is π .

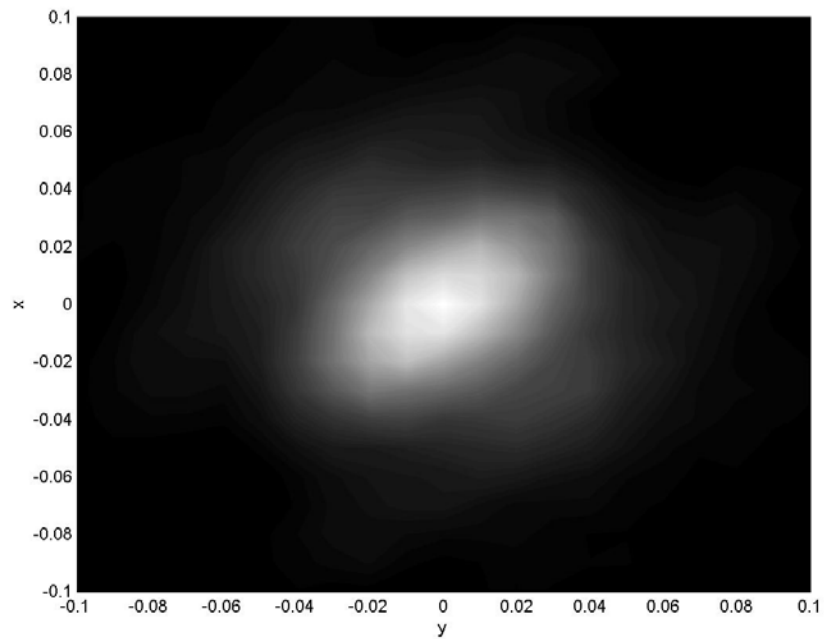


Figure 4-7 : Laser Intensity profile of FSO system using 1550nm wavelength laser for a 3000m propagation distance. Random source phase included and expansion coefficient is 2π .

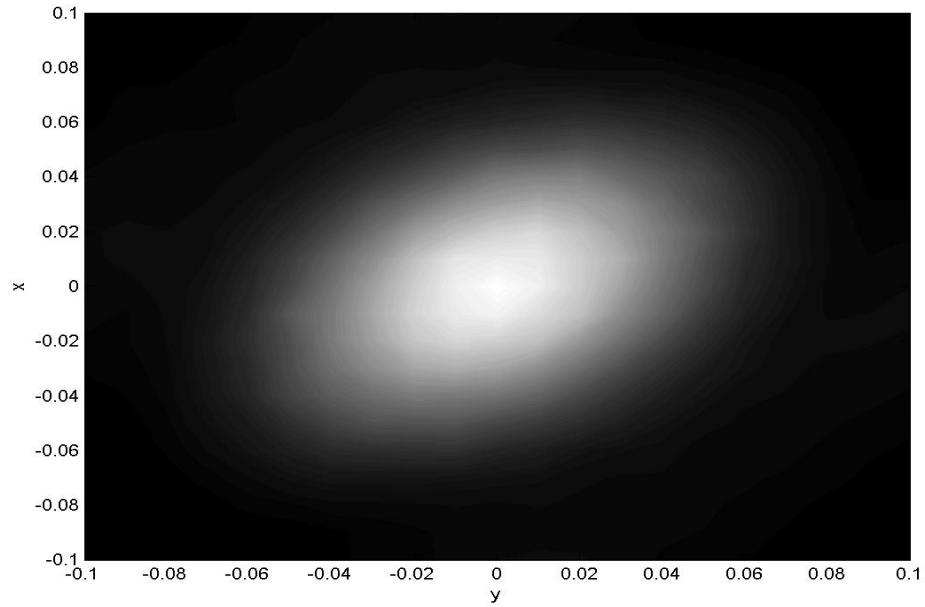


Figure 4-8 : Laser Intensity profile of FSO system using 1550nm wavelength laser for a 5000m propagation distance. Random source phase included and expansion coefficient is π .

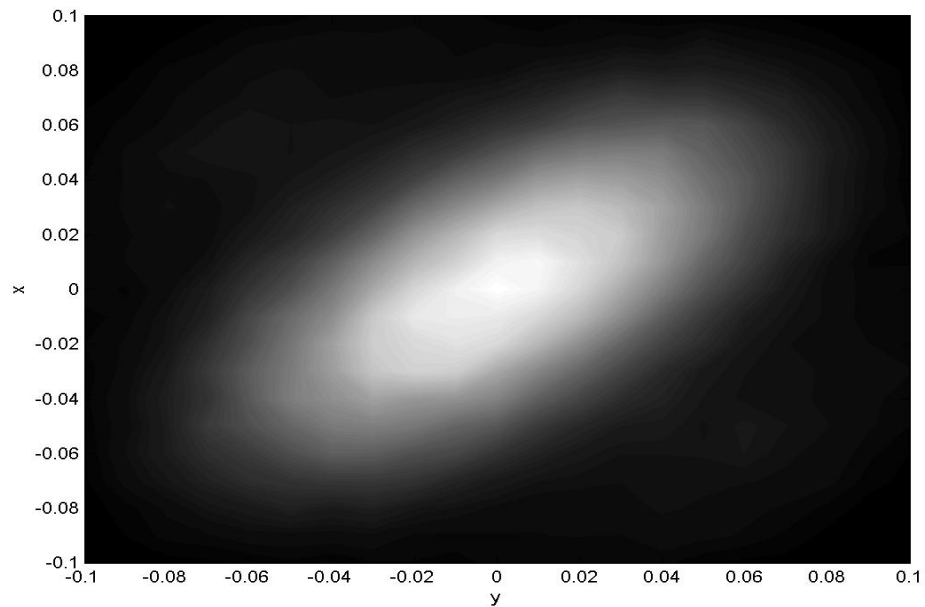


Figure 4-9 : Laser Intensity profile of FSO system using 1550nm wavelength laser for a 5000m propagation distance. Random source phase included and expansion coefficient is 2π .

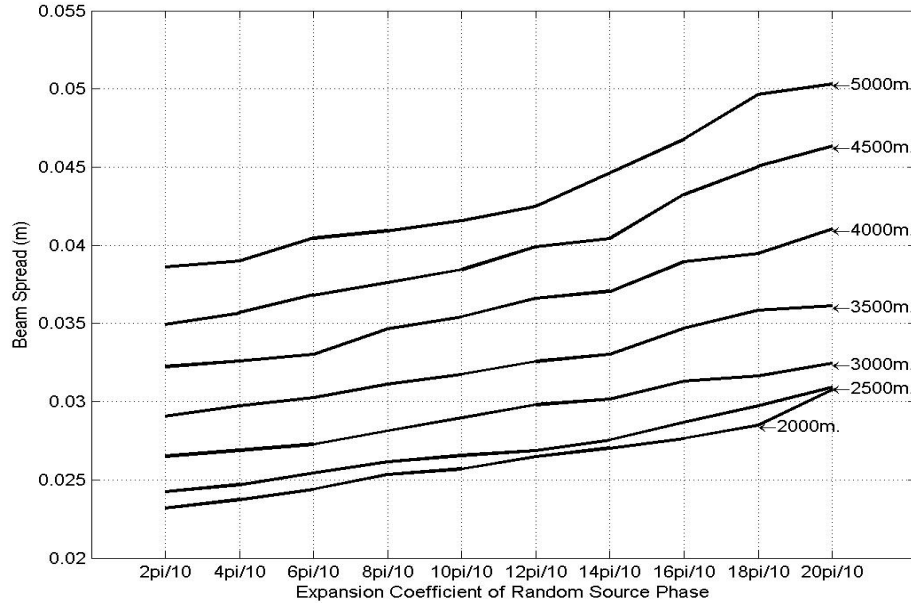


Figure 4-10 : Comparison of laser beam spread of FSO system using 1550nm wavelength laser for a 2000m-5000m propagation distance due to the expansion coefficient of the random source phase.

In figures 4-11 to 4-16, both spatial random source phase and atmospheric turbulence are included in the field integral. The evaluation process is repeated for same propagation distances. In each evaluation, the expansion coefficients of the spatial random source phase is changed from 0-to- 2π , and the values for the parameters of atmospheric turbulence are selected as discussed in section 3.5. In this case also, the increase in the expansion coefficient or the magnitude of the phase values of the spatial random phase has an increasing effect on the beam spread as seen in figure 4-17, but this case has a greater increase in beam spread than the case in which the atmospheric turbulence is not included. In figure 4-17, the graphs of the propagation distances 2000m, 2500m and 3000m are intersecting each other because of the insufficient number of samples used in the simulation because of long run-time problem. The shape of the intensity profile also fluctuates but with a higher fluctuation.

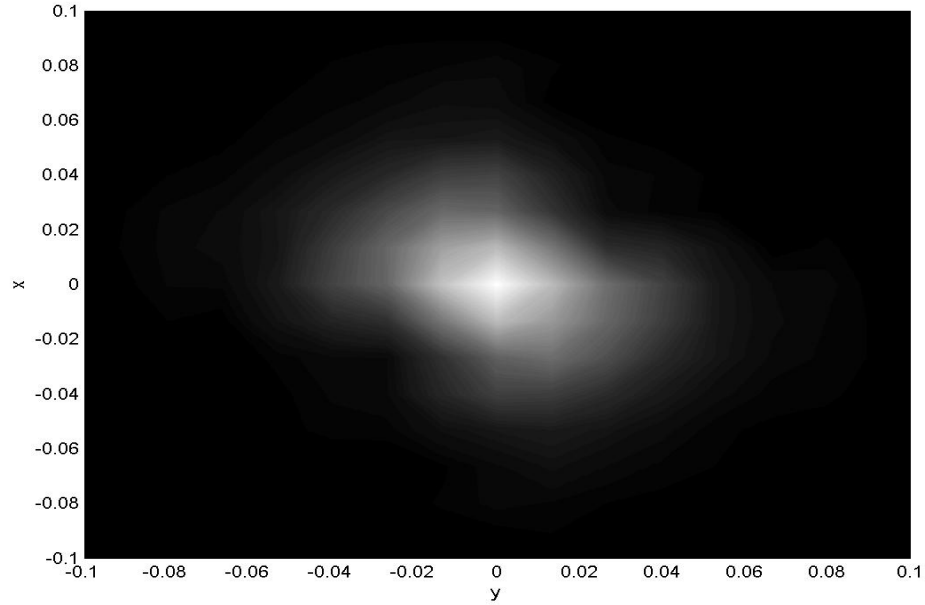


Figure 4-11 : Laser Intensity profile of FSO system using 1550nm wavelength laser for a 2000m propagation distance. Random source phase included and expansion coefficient is π . Atmospheric turbulence is included.

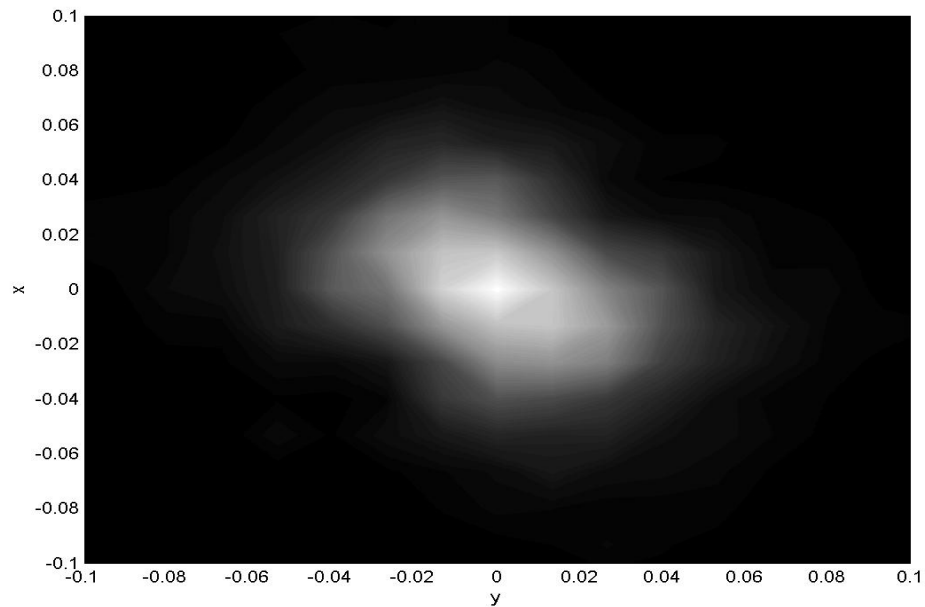


Figure 4-12 : Laser Intensity profile of FSO system using 1550nm wavelength laser for a 2000m propagation distance. Random source phase included and expansion coefficient is 2π . Atmospheric turbulence is included.

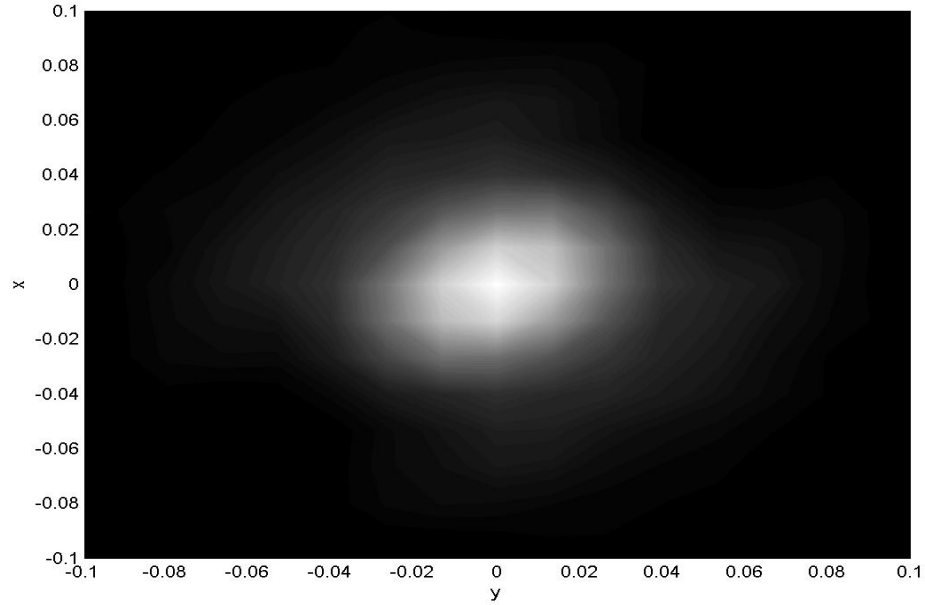


Figure 4-13 : Laser Intensity profile of FSO system using 1550nm wavelength laser for a 3000m propagation distance. Random source phase included and expansion coefficient is π . Atmospheric turbulence is included.

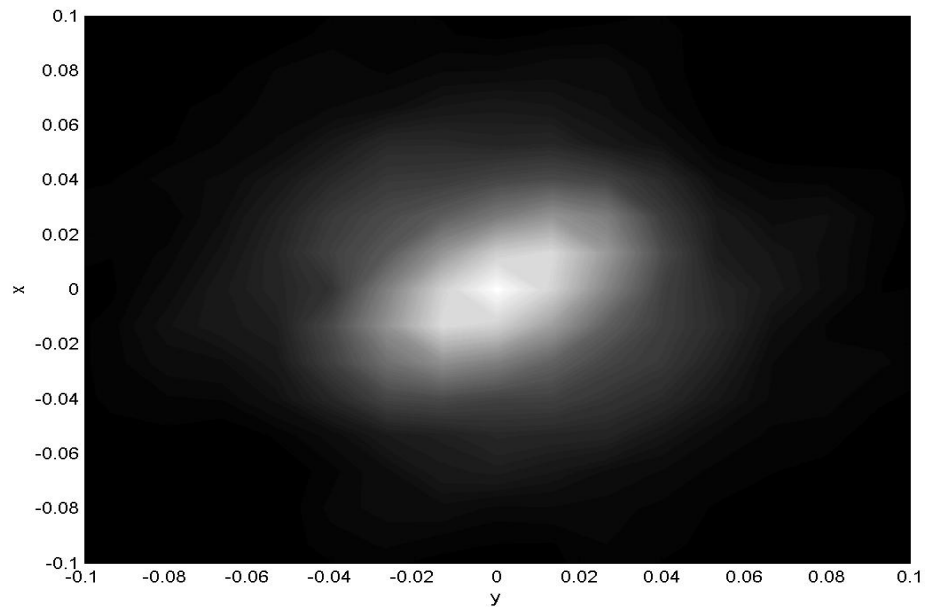


Figure 4-14 : Laser Intensity profile of FSO system using 1550nm wavelength laser for a 3000m propagation distance. Random source phase included and expansion coefficient is 2π . Atmospheric turbulence is included.

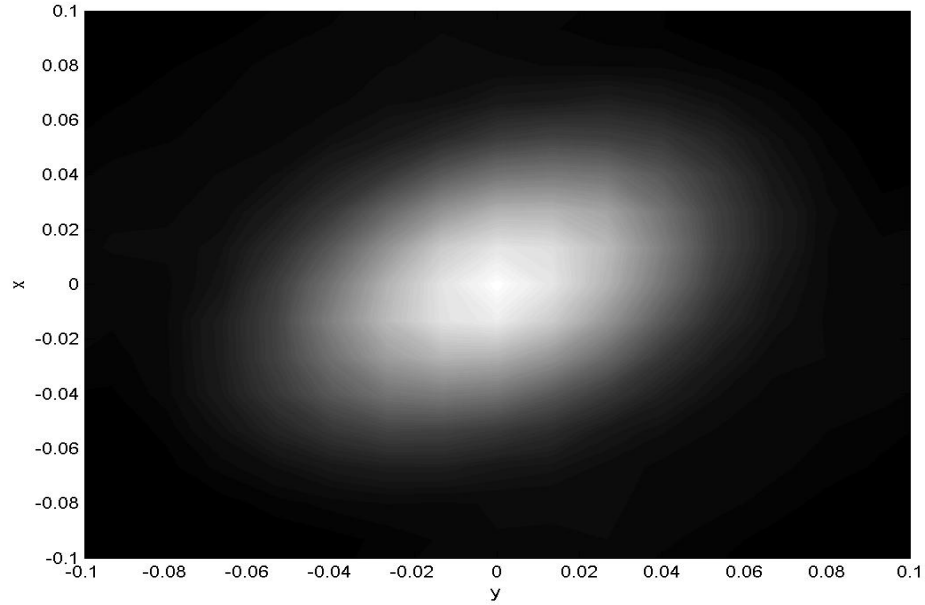


Figure 4-15: Laser Intensity profile of FSO system using 1550nm wavelength laser for a 5000m propagation distance. Random source phase included and expansion coefficient is π . Atmospheric turbulence is included.

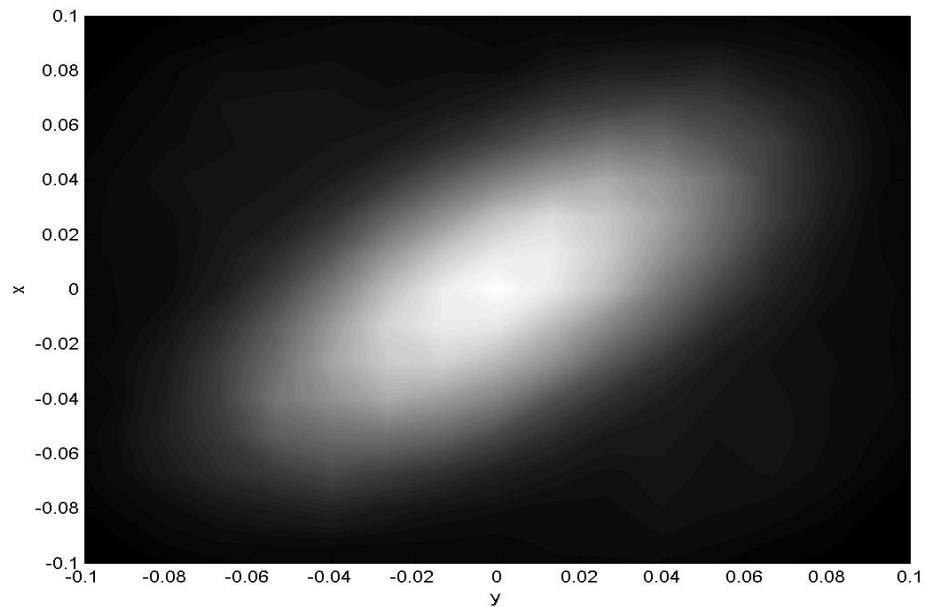


Figure 4-16: Laser Intensity profile of FSO system using 1550nm wavelength laser for a 5000m propagation distance. Random source phase included and expansion coefficient is 2π . Atmospheric turbulence is included.

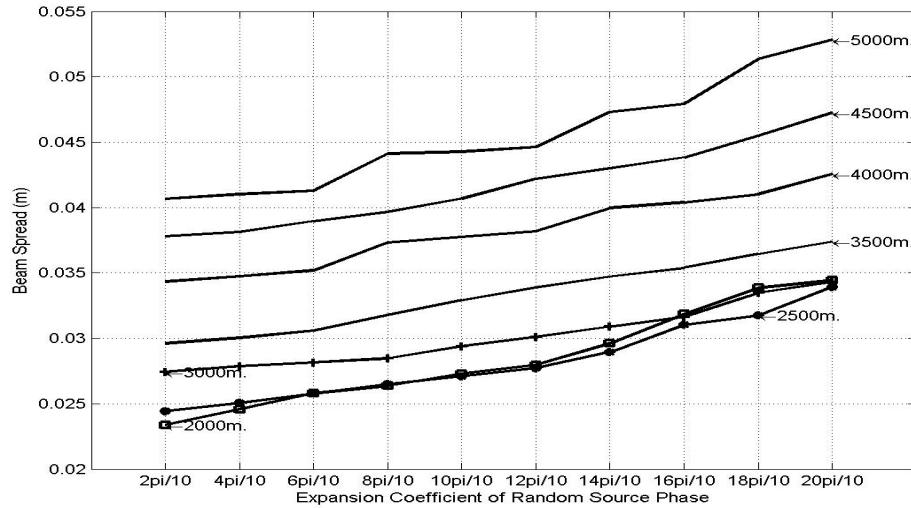


Figure 4-17 : Comparison of laser beam spread of FSO system using 1550nm wavelength laser for a 2000m-5000m propagation distance due to the expansion coefficient of the random source phase.

Figures 4-18, 4-19 and 4-20 illustrate the beam spread of the laser due to the expansion coefficient of the spatial random source phase for each propagation distance discussed above in a comparative manner. As it can be seen in each figure that, higher the expansion coefficient or the magnitude of the spatial random source phase, larger the beam spread and also longer the propagation distance, larger the beam spread. Additionally, the effect of atmospheric turbulence on beam spread can be easily seen from the figures that it further increases the beam spread, so on each point, atmospheric turbulence introduced cases have larger beam spread values than speckle (absence of atmosphere) cases. In case like figure 4-18, as the expansion coefficient of the spatial random phase increases the difference between the beam spread values of atmospheric turbulence and speckle case shall increase. But figures 4-19 and 4-20 do not match in this manner. The reason for this may be the reductive affect of the spatial random phase and the complex part of the atmospheric turbulence on each other. Also another reason may be the insufficient number of samples used in the simulation because of the long run-time problem.

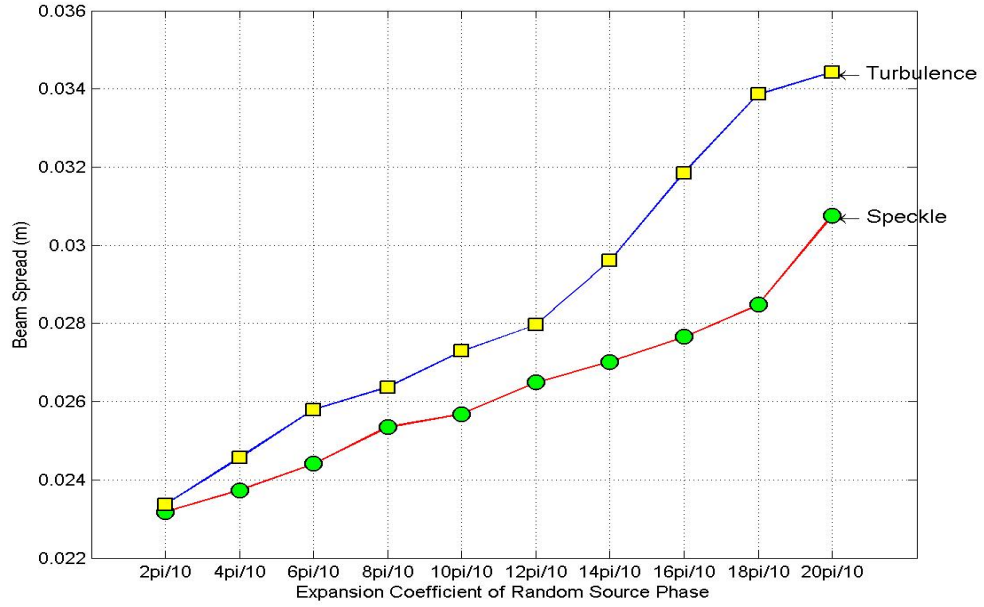


Figure 4-18 : Comparison of laser beam spread of FSO system for random source phase with atmospheric turbulence and random source phase without atmospheric turbulence for a 2000m propagation distance due to the expansion coefficient of the random source phase.

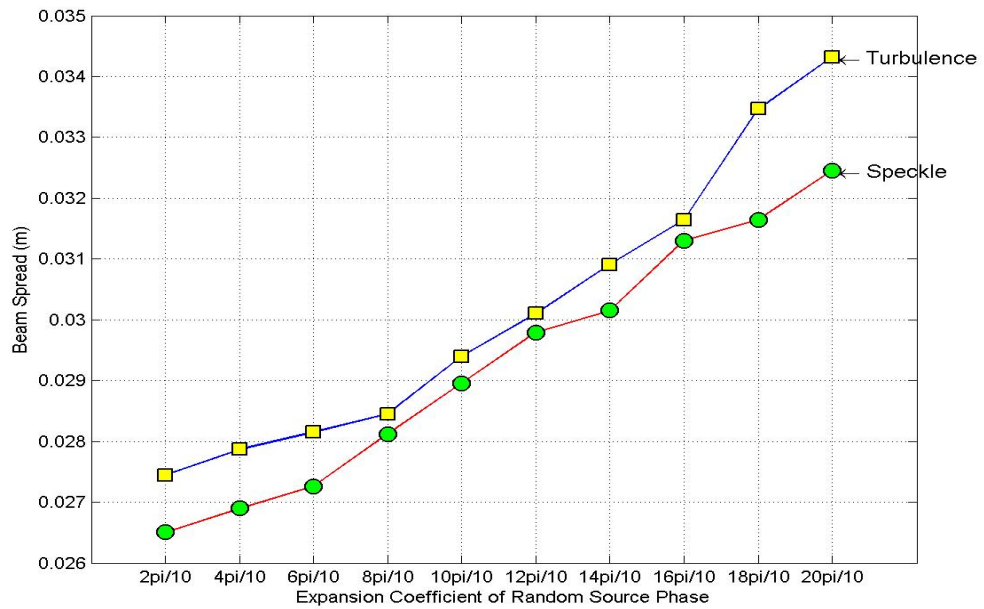


Figure 4-19 : Comparison of laser beam spread of FSO system for random source phase with atmospheric turbulence and random source phase without atmospheric turbulence for a 3000m propagation distance due to the expansion coefficient of the random source phase.

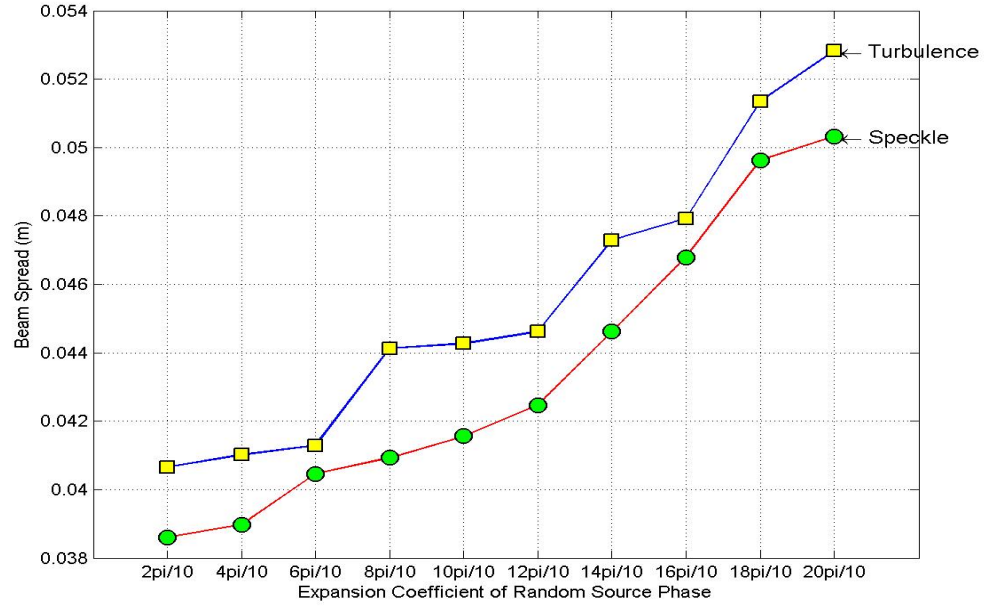


Figure 4-20 : Comparison of laser beam spread of FSO system for random source phase with atmospheric turbulence and random source phase without atmospheric turbulence for a 5000m propagation distance due to the expansion coefficient of the random source phase.

CHAPTER 5

CONCLUSION

The measure of performance of a digital communication system is the **BER (Bit Error Rate)** during data transfer. Since FSO systems are digital communication systems, in order to examine the performance of the system, the parameters affecting BER should be determined.

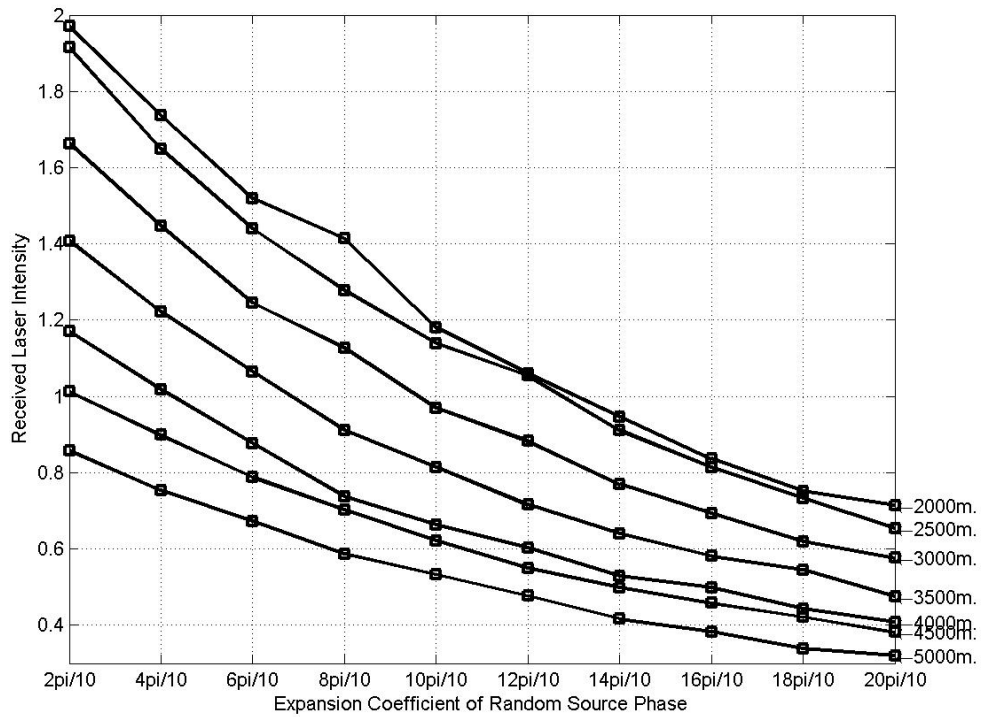


Figure 5-1 : Comparison of laser intensity on receiver site due to expansion coefficient of the spatial random source phase for propagation distances from 2000m up to 5000m.

In wireless systems, one of the important factors affecting BER of the system is the signal level at the receiver site. In FSO systems, because the carrier signal is an infrared laser, and the measure of the level of the laser signal is its received intensity [2], in this study, effects of spatial random source phase and atmospheric turbulence on intensity profile on receiver site are examined.

Figure 5-1 illustrates the received laser intensity of a system that both spatial random source phase and atmospheric turbulence are introduced, according to both the expansion coefficient / magnitude of the spatial random source phase and the propagation distance. The intensity levels in figure 5-1 are evaluated at $2^{-1/2}$ times the maximum intensity values. As it can be seen from the figure that the signal intensity at the receiver site has a decreasing trend as the expansion coefficient of the spatial random source phase increases. This is because the increase in the expansion coefficient or magnitude causes increase in the beam spread which reduces the intensity of the beam and also the loss of the shape of the beam intensity profile has a negative affect on the level of received intensity. The above discussions show us that the performance of a FSO system is negatively affected from the increase in expansion coefficient or magnitude of the spatial random source phase. Also it can easily be seen that increase in the propagation distance causes decrease in the received laser intensity. Therefore it also has a negative effect on the performance of the FSO system.

The main parameters of the field integral that are directly proportional to the laser intensity profile and that can be controlled by the users are the size of the laser source, the amplitude of the field and the propagation distance. This is because, larger the size of the laser source, smaller the beam spread, also higher the amplitude of the transmitted laser, higher the level of received intensity. But these

parameters are limited by the laser safety restrictions and mainly by the cost of the link. If the system is deployed for shorter propagation distances, the system performance can be increased. This can be done by using repeaters having amplifying property. But adding repeaters will cause a decrease in the data rate of transmission because in each repeater the signal is transformed from light to electricity and electricity to light. This process is very slow as compared with the full optic transmission links.

Future work related to this study can be the examination of the intensity fluctuations by using a similar simulation, however this time applied to the fourth order moments.

REFERENCES

- [1] **LIU, Q., QIAO C., MITCHELL, G., STANTON, S.**, (2005) Optical Wireless Communication Networks For First- And Last-Mile Broadband Access [Invited], *J. Opt. Net.* Vol. 4, pp. 807-828.
- [2] **PRATT, W.K.**, (1969), *Laser Communication Systems*, John Wiley & Sons, NY.
- [3] **BLOOM, S.**, (2001) The Physics of Free-Space Optics, AirFiber Inc., 802-0006-000 M-A1.
- [4] **STROUD, P.D.**, (1993) Diffraction and Scintillation of Laser Beams by Atmospheric Turbulence, Los Alamos National Lab Report, LAUR-93-1401.
- [5] **BOOKNER, E.**, (1970) Atmospheric propagation and communication channel model for wavelengths, *IEEE Trans. Commun. Technol.*, Vol. COM-18, pp. 396-416.
- [6] **BORN, M., WOLF, E.**, (1970), *Principles of Optics: Electromagnetic Theory of Propagation, Interference and Diffraction of Light*, Pergamon Press, NY.
- [7] **KLEIN, M.V.**, (1970), *Optics*, John Wiley & Sons, NY.
- [8] **FANTE, R.L.**, (1975) Electromagnetic Beam Propagation in Turbulent Media, *Proceedings of The IEEE*, Vol.63, pp.1669-1692.
- [9] **SALEM, M., SHIRAI, T., DOGARIU, A., WOLF, E.**, (2003) Long-Distance Propagation of Partially Coherent Beams Through Atmospheric Turbulence, *Optics Communications*, Vol. 216, pp.261-265.
- [10] **KHMELEVSTOV, S.**, (1973) Propagation of Laser Radiation in A Turbulent Atmosphere, *Appl. Opt.*, Vol. 12, pp. 2421-2432.
- [11] **TATARSKII, V.I.**, (1961), *Wave Propagation in A Turbulent Medium*, McGraw-Hill, NY.

- [12] **ANDREWS, L.C., PHILLIPS, R.L.**, (1998), *Laser Beam Propagation Through Random Media*, SPIE Press, Washington.
- [13] **ANDREW, L.C.** et. al., (2001), *Laser Beam Scintillation with Applications*, SPIE Press, Washington.
- [14] **KREYSZIG E.**, (1999), *Advanced Engineering Mathematics*, John Wiley & Sons, NY.
- [15] **PRESS, W.H.** et. al., (1992), *Numerical Recipes in C: The Art of Scientific Computing*, Cambridge University Press, NY.

APPENDIX A : Intensity Profile

```
%-----  
%%%%%%%%%%%%%%%%%%%%%%%%%%%%%%%%%%%%%%%%%%%%%%%%%%%%%%%%  
%-----  
%  
%Clear Workspace, Clear Scr & Close Windows  
%  
clear all;  
clc;  
close all;  
%  
%  
%-----  
%%%%%%%%%%%%%%%%%%%%%%%%%%%%%%%%%%%%%%%%%%%%%%%%%%%%%%%%  
%-----  
%  
%Declaration of the global variables of the integrand of FIELD Uxyz  
%  
global A;%The amplitude of the square aperture  
global k;%Wave Number  
global x;%Coordinate on source plane  
global y;%Coordinate on source plane  
global z;%Propagation Distance  
global j;%Complex "i" <--> "sqrt(-1)"  
global alpha_s;%source size  
%
```

```

%-----
%%%%%%%%%
%-----
%
%Assignment of variables
%
lambda=1.55*1e-6;%The wave length of light
k=(2*pi)/lambda;%Wave number
j=sqrt(-1);%Complex number
A=1;%The amplitude of the light beam at source
N=32;%Number of integration points
alpha_s=0.05;%The size of the source
%
%-----
%%%%%%%%%
%-----
%
%Gaussian Integration Weights
%
lowerLimit=-alpha_s;
upperLimit=alpha_s;
[Xo,Wx] = gaussquad(N, lowerLimit, upperLimit);
[Yo,Wy] = gaussquad(N, lowerLimit, upperLimit);
M=10;%number of instants
C=20;%number of (x,y) coordinates
axis_limit=2;
X=(axis_limit*lowerLimit):(2*axis_limit*upperLimit/C):(axis_limit*upperLimit);

```

```

Y=(axis_limit*lowerLimit):(2*axis_limit*upperLimit/C):(axis_limit*upperLimit);
save('X','X');
save('Y','Y');
save('C','C');
save('M','M');
%
%-----
%%%%%%%%%
%-----
%
%The loop for propagation distance
for z=2000:500:5000
%
%-----
%%%%%%%%%
%-----
%
%The loop of variance of random phase
for sigma_2=0:pi/5:2*pi % The variance of the phase
%
%-----
%%%%%%%%%
%-----
%
%The loop of the coordinates (x,y)
I=zeros(C+1,C+1);
for y_index=1:C+1

```



```

y=Y(y_index);
for x_index=1:C+1
    y_index
    x_index
    x=X(x_index);
%
%-----
%%%%%%%%%
%-----
%
%The loop of the instants
for instant=1:M
%
%-----
%%%%%%%%%
%-----
%
%Random phase have a(uniform distribution)
phase=sqrt(sigma_2)*(rand(N,N)-0.5);
%
%-----
%%%%%%%%%
%-----
%
%Integration
Uxyz=0;%The initial value of the field before integration
for y0=1:N

```

```

for x0=1:N
    Uxyz=Uxyz+integrand(Xo(x0),Yo(y0),phase(x0,y0))*Wx(x0)*Wy(y0);
end
end
I(y_index,x_index)=I(y_index,x_index)+Uxyz*conj(Uxyz);
%
%-----
%%%%%%%%%
%-----
%
%END OF THE INSTANT LOOP
end
%
%-----
%%%%%%%%%
%-----
%
%END OF THE COORDINATE LOOPS
end
end
%-----
%%%%%%%%%
%-----
%
%SAVE WORKSPACE FOR POWER FAILURE
%Saving Intensity values
%
fileName=['speckle' num2str(sigma_2) '_' num2str(z)];

```

```

save(fileName,'I');
%
save workspace;
%
%-----
%%%%%%%%%
%-----
%
figure(1)
colormap gray
contourf(Y,X,I/M,150);
xlabel('y');
ylabel('x');
hold on;
contour(Y,X,I/M,150);
hold off;
%
%-----
%%%%%%%%%
%-----
%
FILE_NAME=['speckle' num2str(sigma_2) '_' num2str(z)];
saveas(gcf, FILE_NAME,'jpg')
%
%-----
%%%%%%%%%
%-----

```

```
%  
%END OF THE VARIANCE LOOP  
end  
%-----  
%%%%%%%%%  
%-----  
%  
%END OF THE PROPAGATIN LOOP  
end
```

APPENDIX B : Field Integrand

```
function ret=integrand(Xo,Yo,Q)
%-----
%
%Defined variables of integrand of Uxyz
global A;
global k;
global x;
global y;
global z;
global limit;
global j;
%
%-----
%
%Definition of Integrand
ret=(k/(2*pi*j*z))*...
    A*...
    exp(((j*k)/(2*z))*(y-Yo)^2)*...
    exp(((j*k)/(2*z))*(x-Xo)^2)*...
    exp(j*Q*(Xo+Yo));
%
%-----
%
```

APPENDIX C : Gauss Quad

```
function [xx, ww] = gaussquad(n, a, b)
% Check number of input arguments.
error(nargchk(1, 3, nargin));

% Assign default values to missing arguments.
switch nargin
    case 1
        % GAUSSQUAD(N)
        b = 1;
        a = -1;
    case 2
        % GAUSSQUAD(N, C)
        b = a;
        a = 0;
end

u = 1 : n-1;
u = u ./ sqrt(4*u.^2 - 1);

% Same as A = diag(u, -1) + diag(u, 1), but faster (no addition).
A = zeros(n, n);
A( 2 : n+1 : n*(n-1) ) = u;
A( n+1 : n+1 : n^2-1 ) = u;

% Find the base points X and weight factors W for the interval [-1,1].
[v, x] = eig(A);
[x, k] = sort(diag(x));
```

```
w = 2 * v(1,k).^2;
```

```
% Linearly transform from [-1,1] to [a,b].
```

```
x = (b - a) / 2 * x + (a + b) / 2; % transform base points X
```

```
w = (b - a) / 2 * w; % adjust weights
```

```
% If output arguments are given, return output and exit.
```

```
if nargout
```

```
    xx = x;
```

```
    ww = w;
```

```
    return
```

```
end
```

APPENDIX D : Intensity Level

```
%Amount of Spread Due to Phase Variance
%-----
%%%%%%%%%
%-----
clc;
clear all;
close all;
%
%-----
%%%%%%%%%
%-----
%
load('X','X');
load('Y','Y');
load('C','C');
load('M','M');
%
%-----
%%%%%%%%%
%
for z=2000:500:5000
sigma_index=0;
for sigma_2=0:pi/5:2*pi
```



```

    sigma_index=sigma_index+1;
fileName=['speckle' num2str(sigma_2) num2str(z)];
load(fileName,'I');
%
%-----
%%%%%%%%%
%-----
%
MAX=max(max(I/M));
pow=MAX/exp(2);
error=7;
for i=1:C+1
    for j=1:C+1
        if pow-error*pow/100<I(i,j)/M & I(i,j)/M<pow+error*pow/100
            spread(sigma_index)=(sqrt((X(i))^2+(Y(j))^2));
        end
    end
end
%
%-----
%%%%%%%%%
%-----
%
end
fileName=['SPECKLE_SPREAD' num2str(z)];
save(fileName,'spread');
%
```

```

%-----
%%%%%%%%%
%-----
%

figure(1)
PI=0:2*pi/10:2*pi;
plot(PI(2:11),spread(2:11))
set(gca,'XTick',PI(2:11))
set(gca,'XTickLabel',{'2pi/10','4pi/10','6pi/10','8pi/10','10pi/10','12pi/10','14pi/10','
16pi/10','18pi/10','20pi/10'})
ylabel('Beam Spread(m.)')
xlabel('\sigma^2 (Variance of Source Phase)')
FILE_NAME=['speckle_spread' num2str(z)];
saveas(gcf, FILE_NAME,'jpg')
%
%-----
%%%%%%%%%
%-----
end

```

APPENDIX E : Comparison

```
%Comperative Spread Due To Distance
%
%-----
%%%%%%%%%
%-----
%
clc;
clear all;
close all;

%
%-----
%%%%%%%%%
%-----
%
i=0;
for distance=2000:500:5000
    i=i+1;
    fileName=['speckle_spread' num2str(distance)];
    load(fileName,'spread');
%
%-----
%%%%%%%%%
%-----
```

```

%
X_AXIS=0:pi/5:2*pi;
ARROW=['\leftarrow' num2str(distance) 'm'];
figure(1)
xlabel('\sigma^2 (Variance of Source Phase)')
ylabel('Beam Spread (m)')
plot(X_AXIS(2:11),spread(2:11),'k')
grid on
title('Comparison of Spread Due to Distance')
text(X_AXIS(10),spread(10),ARROW,...
      'HorizontalAlignment','left','FontSize',18)

set(gca,'XTick',PI(2:11))
set(gca,'XTickLabel',{'2pi/10','4pi/10','6pi/10','8pi/10','10pi/10'...
                     '12pi/10','14pi/10','16pi/10','18pi/10','20pi/10'})
hold on
end
FILE_NAME=['comparison'];
saveas(gcf, FILE_NAME,'jpg')
%
%-----
%%%%%%%%%
%-----

```